

Highlights

ActVAE: Modelling human activity schedules with a deep conditional generative approach

Fred Shone, Tim Hillel

- Introduce ActVAE generative model for activity schedules conditioned on input labels.
- Combines explicit generation of structured latent models with conditionality.
- Model can be used within new and existing demand modelling frameworks.
- Extend model evaluation using joint density estimation of schedules and labels.
- Outputs diverse & realistic schedules which reflect label–schedule relations.

ActVAE: Modelling human activity schedules with a deep conditional generative approach

Fred Shone^a, Tim Hillel^{a,*}

^a*Department of Civil, Environmental and Geomatic Engineering, University College London, UK*

Abstract

Modelling the complexity and diversity of human activity scheduling behaviour is inherently challenging. We demonstrate a deep conditional-generative machine learning approach for the modelling of realistic activity schedules depending on input labels such as an individual's age, employment status, or other information relevant to their scheduling. We combine (i) a structured latent generative approach, with (ii) a conditional approach, through a novel Conditional VAE architecture. This allows for the rapid generation of precise and realistic schedules for different input labels. We extensively evaluate model capabilities using a joint density estimation framework and several case studies. We additionally show that our approach has practical data and computational requirements, and can be deployed within new and existing demand modelling frameworks. We evaluate the importance of generative capability more generally, by comparing our combined approach to (i) a purely generative model without conditionality, and (ii) a purely conditional model which outputs the most likely schedule given the input labels. This comparison highlights the usefulness of explicitly modelling the randomness of complex and diverse human behaviours using deep generative approaches.

Keywords: Activity based models, Activity schedules, Conditionality, Generative learning, Deep learning, Machine learning, Variational Auto-encoders

1. Introduction

We consider the modelling of human activity schedules based on input labels, such as household size, car ownership and socio-economic attributes. For this work, we define an activity schedule as a sequence of activity participations, with associated durations, belonging to an individual. Human activity schedules result from a complex combination of processes, including: (i) constraints, such as needing to fit all activities within a given time budget, (ii) preferences, such as wanting to visit a friend or spend longer shopping, and (iii) interactions, both with each other and the environment, such as within a household or with traffic. Modelling realistic and representative activity schedules is therefore inherently challenging.

*Corresponding author

Email addresses: `frederick.shone.17@ucl.ac.uk` (Fred Shone), `tim.hillel@ucl.ac.uk` (Tim Hillel)

Our first contribution is to introduce a conditional-generative model called ActVAE. ActVAE is described in Section 6 and comprehensively evaluated against two baseline approaches in Section 7, where we show the model is able to best generate realistic schedules and distributions of schedules. Unlike previous work in the literature, we incorporate a structured latent generative approach, the Variational Auto-Encoder (VAE). Compared to previous schedule synthesis work using a VAE (Shone and Hillel, 2025), we add conditional capability, so that the model can predict changes to scheduling due to changes in input labels, allowing schedules to be tailored to different individuals, and therefore enabling simulation of counterfactual scenarios, such as changing mobility due to an ageing population or other demographic or economic changes. This makes the approach viable within new and existing applied modelling frameworks, which otherwise rely on complex compositions of sub-models to generate schedules. In addition to the convenience of combining multiple components into a joint scheduling model, our approach allows for more precise and diverse schedule modelling, important for equitable representation of human behaviours.

Secondly, we compare ActVAE to a purely *generative* baseline model (i.e. without conditionality) and a purely *conditional* baseline model that outputs the most likely schedule given the input labels. We use the *conditional* model to represent the capability of existing applied approaches, which do not use a generative approach. The key distinction is that *conditional* approaches seek to map different schedules to different input labels directly. In contrast, we use and compare to an *explicit generative* approach that explicitly models schedules as a random distribution without conditionality. We use this experiment to demonstrate and quantify the capability of the explicit generative versus traditional conditional approaches. Perhaps unsurprisingly, given the complexity and diversity of human scheduling, we find that explicit modelling of randomness outperforms the purely conditional approach.

For this work, we consider 24-hour-long activity schedules, starting and ending at midnight, but the technique could be generalised to any total duration or period with appropriate input data. We do not consider activity locations or associated trips between activities, instead incorporating outbound travel into the corresponding activity.

This document’s structure is summarised in Table 1. Note that we make extensive use of appendices to provide additional evidence for our findings whilst keeping the main manuscript concise. All experiments are reproducible using code added to the open-source software Caveat¹.

2. Literature review

In this section, we first define a taxonomy of approaches for modelling activity scheduling, covering four axes: (i) theory versus data-driven, (ii) compositional versus joint, (iii) conditional versus non-conditional, and (iv) implicit versus explicit generative. We then review existing literature using our taxonomy.

2.1. Activity scheduling model taxonomy

We review existing activity scheduling models (including applied frameworks that incorporate activity scheduling) using the following taxonomy, with an overview of key

¹<https://github.com/big-ucl/caveat>

Table 1: Summary of contents

Section 2	Taxonomy and review of existing literature
Section 3	Motivations for our approach to activity scheduling
Section 4	Variational Auto-Encoder (VAE) theory
Section 5	Methodology
Section 6	Model design
Section 7	Results
Section 8	Conclusions and further work
Appendix A	The challenge of conditional VAE disentangling through a mutual information perspective
Appendix B	Alternative generative model designs and evaluations (CatVAE, VQVAE & SWAE)
Appendix C	ActVAE architecture ablation study (model architecture selection)
Appendix D	Mutual information estimation methodology
Appendix E	Detailed joint density estimation studies
Supplementary case studies (Appendix F):	
Appendix F.1	Forecasting demonstration (using real NOMIS data)
Appendix F.2	Data availability case study
Appendix F.3	Labels availability case study
Appendix F.4	Foundational model case study

Table 2: Taxonomy of existing activity scheduling approaches

Model	Approach	Taxonomy			
CEMPDAP (Sener et al., 2006)	econometric	theory-driven	compositional	conditional	NA
DaySim (Bradley et al., 2010)	econometric	theory-driven	compositional	conditional	NA
WGAN (Badu-Marfo et al., 2020)	GAN	data-driven	joint	conditional	implicit
SALT (Hafezi et al., 2021)	decision trees	data-driven	compositional	conditional	NA
SDS (Khan and Habib, 2023)	econometric	theory-driven	compositional	conditional	NA
OASIS (Pougala et al., 2023)	optimisation	theory-driven	joint	conditional	NA
Conditional RNN (Koushik et al., 2023)	RNN	data-driven	joint	conditional	NA
Act2Loc (Liu et al., 2024)	autoregression	data-driven	joint	conditional	explicit
ContRNN (Shone and Hillel, 2025)	VAE	data-driven	joint	non-condit.	explicit
ActVAE (this paper)	VAE	data-driven	joint	conditional	explicit

identified prior works presented in Table 2.

2.1.1. Theory versus data-driven

Theory-based (also *hand-designed* or *model-based*) approaches use interpretable models intended to incorporate the knowledge of the modeller, through their functional form and sometimes via manual calibration of the parameters themselves. *Data-driven* approaches instead use large, flexible, and typically less interpretable, functional forms and rely more heavily on data to learn or estimate the required mappings. In practice, models fall on a spectrum between theory-driven and data-driven; even heavily data-driven approaches, such as deep learning, use prior experience and domain knowledge to help specify architectures. For example, recurrent architectures are typically used for language problems, and convolutions for image problems. However, data-driven approaches to activity scheduling are relatively new, and therefore, such prior experience and domain knowledge are limited.

2.1.2. *Compositional versus joint*

Compositional models split the scheduling process into component models, such as primary tour choice, secondary tour choice and so on, each trained and or calibrated separately. *Joint* models generate schedules without this decomposition, instead considering all choice dimensions jointly. The key distinction is that whereas a *joint* model is estimated and/or calibrated end-to-end, for example by minimising a combined loss function, a sequential approach is estimated and/or calibrated component by component.

2.1.3. *Conditional versus non-conditional*

Conditional models generate outputs conditioned on one or more input labels, such as socio-economic variables, allowing for schedules to be tailored to different individuals or population segments. *Non-conditional* models instead use a generic sampling approach which approximates the distribution of the whole modelled population.

2.1.4. *Implicit versus explicit generative*

Unlike discriminative models, which aim to map inputs to a well-defined target, such as a discrete choice, *generative models* instead seek to model a target distribution that is only partially observed. In our case, the target distribution is the real distribution of activity schedules and labels. Generative models are therefore capable of outputting novel (previously unobserved) data. We detail in Section 3.1 why activity scheduling should be considered as a generative problem.

Although all approaches in Table 2 can be used to generate new schedules, only those that directly approximate the schedule distribution through end-to-end training are considered to be generative models. We further categorise the generative approaches into *explicit* generative and *implicit* generative, following Bond-Taylor et al. (2022). *Explicit* generative models specify a probability density function which is fit (on training data) to directly approximate the target distribution. In contrast, *implicit* generative models do not define a density function. Instead, they define a sampling procedure which is fit to produce samples that match the target distribution.

2.2. *Evaluation of the literature*

2.2.1. *Traditional compositional approaches*

The current prevalent approach to activity scheduling, employed in CEMDAP (Sener et al., 2006), DaySim (Bradley et al., 2010) and SDS (Khan and Habib, 2023), relies on *econometric* frameworks. These *econometric* approaches decompose the scheduling process into a series of choice components, each typically addressed by a discriminative theory-driven model or rule-based model. Whilst not trained end-to-end, compositional approaches attempt to model a realistic distribution of schedules (often with manual recalibration of the individual components) and can generate novel outputs.

Each of these papers uses observed data to fit unknown parameters, but they first make many assumptions about the availability and structure of the decomposed choices. Notably, they typically limit participation patterns to common tours, discretise time steps into imprecise periods, and simplify complex joint relationships into decomposed steps.

We describe these approaches as *theory-driven*, *compositional*, and *conditional*. We do not treat these models as generative as they do not explicitly model the *joint* target distribution.

2.2.2. Optimisation approaches

Unlike the above *compositional* approaches, the *simulation* approach in OASIS (Pougala et al., 2023) seeks to *jointly* model activity schedules (and locations and modes) consistent with behavioural theory using a utility optimisation approach. Compared to compositional approaches, the *joint* nature of OASIS allows it to better consider joint distributions. However, estimation of the parameters and simulation of schedules is computationally expensive, limiting scalability. Manser et al. (2021) manage to scale the approach to application as part of an activity-based transport demand model, but they limit the scope of the simultaneous approach to activity timings only. Rezvany et al. extend the framework to modelling household schedules, but the increased complexity further limits scalability.

2.2.3. Machine learning approaches

Initial machine learning (ML) based approaches to activity scheduling have also adopted *compositional* approaches, replacing the theory-driven components with more *data-driven* alternatives, such as classification models, e.g. for sequence prediction (Nayak and Pandit, 2023) and duration prediction (Hafezi et al., 2021).

ML approaches to discrete choice problems have been shown to scale to massive choice sets (Salvadé and Hillel, 2025). This makes the combination of decomposed choices, such as location and mode, into single joint or simultaneous choices feasible. However, this has not yet been extended to activity schedule modelling, which can be thought of as the simultaneous choice of all daily activity participations and their timings.

Most recently, deep machine learning approaches, such as the deep recurrent network (RNN) by Koushik et al. (2023), provide a *joint data-driven* architecture for generating activity schedules. We refer to this model as a conditional RNN in Table 2 and use a variation of it as a baseline in our experiments. We classify the conditional RNN as *joint* because it is trained end-to-end using a single loss function. Unlike a standard (explicit generative) auto-regressive approach, the model does not incorporate random (i.e. Monte-Carlo) sampling during training or generation. Instead, schedules are modelled as a sequence of 10-minute activity participations, with the model outputting softmax probabilities for all activities at each time interval, and each interval then assigned to the most likely activity. This means it outputs a single *most likely* schedule for each combination of input labels. We therefore do not consider this model to be generative.

2.2.4. Deep generative modelling approaches

Deep Generative Models (DGMs) make use of large training datasets and deep machine learning architectures to learn the distributions of complex high-dimensional data such as images (Xu et al., 2018), video (Deng et al., 2025), and text (Devlin et al., 2018). There are many generative approaches, including auto-regressive, Variational Auto Encoders (VAEs) (Kingma and Welling, 2013), Generative Adversarial Networks (GANs) (Goodfellow et al., 2014), Diffusion (Ho et al., 2020), and Normalising Flows (Rezende and Mohamed, 2015).

There have been limited papers that explore deep generative approaches for activity schedule modelling, predominantly with GANs (Badu-Marfo et al., 2020; Kim et al., 2022). GANs use a discriminator model to guide the training of a generator model, potentially allowing for the learning of very complex distributions conditional on input

Table 3: Glossary of probability notation for Section 3

x	schedule
y	labels (conditional data for schedule)
$p(x)$	probability distribution of schedules
$p(x, y)$	joint distribution of schedules and labels
$p(x y)$	conditional distribution of schedules on labels
z	a latent embedding or representation
$p(z)$	the latent prior distribution

labels. However, this *implicit* approach to generation is prone to poor density estimation. This limitation is likely why both papers acknowledge that these models perform poorly at generating schedule distributions. The density estimation capability of GANs is discussed in detail in Section 3.3.1.

In contrast, the autoregressive approach by Liu et al. (2024) is *explicit generative* but uses temporal aggregation and sequence clustering, reducing the ability of the model to represent a realistic diversity of schedules. This simplification is likely required due to the data inefficiency of autoregressive approaches, particularly if sequences are long or their distributions are complex. The suitability of auto-regressive approaches based on data efficiency is discussed in detail in Section 3.3.2.

Most recently, Shone and Hillel (2025) has demonstrated a VAE for generating schedules. The VAE combines an *explicit generative* approach with a data-efficient compressed latent prior. The VAE is therefore able to rapidly generate precise and feasible schedules that are shown to be representative in aggregate using density estimation. However, their *non-conditional* approach does not incorporate any conditionality to input labels, which they describe as schedule *synthesis* rather than modelling. In other words, the model cannot be used to generate activity schedules that reflect differences between different modelling contexts; for example, the schedule for a retired person vs a full-time worker. This is a crucial element of transport demand modelling, as this conditionality is used to model responses to new scenarios such as changes in demographics or transport accessibility.

3. Motivations for our approach to activity scheduling

In this section, we detail why activity scheduling should be considered as a generative, rather than compositional, problem. We then detail why a structured latent model, the Variational Auto-Encoder (VAE), is preferred. Key notation for this section is summarised in Table 3.

3.1. Generative versus discriminative problems

Discriminative models, such as those used to represent individual choice components in compositional activity scheduling frameworks, seek to directly model the conditional probability $p(y|x)$, where y is an output label/s and x some input feature/s. For example, we might seek to predict if an input schedule belongs to someone who has access to a car, where x is a schedule, and y is a car ownership label. However, for this work, we wish to model $p(x|y)$, i.e. the probability of a schedule dependent on input labels. The key distinction between labels y and schedules x is that we can consider all possible values

(i.e. the *space*) of the labels to be known and well defined, whereas that is not the case for the schedule space. In the first case, where we seek to predict an output label, available data typically enumerates all possible output labels, but in the latter case, where we seek to predict schedules, available data does not enumerate all possible schedules. We use this *reversed* notation throughout, i.e. $p(x|y)$, consistent with generative machine learning literature such as [Kingma and Welling \(2013\)](#).

Consider a schedule aggregation of one-hour time steps and only two possible activity types. There are then 2^{24} (over 16 million) possible 24-hour activity schedules. More precise schedule representations, incorporating more activity types and finer temporal steps, quickly approach essentially infinite diversity. In comparison, available datasets of human activity schedules typically contain only tens of thousands of samples. An important consideration for any modeller is therefore whether they wish to generate schedules not previously observed in the limited training data. To do so requires learning the distribution $p(x)$ (or for conditional-generation, $p(x | y)$), i.e. the probability distribution of all possible schedules. This is a distinctly *generative modelling* problem.

3.2. Critique of compositional and autoregressive approaches

We note that traditional *compositional* approaches can be considered as *analogous* to autoregressive generative formulations, in which complex distributions are broken down into sequences of simpler distributions:

$$p(x | y) = \prod_{i=1}^n p(x_i | x_{<i}, y), \quad (1)$$

where x_1, x_2, \dots, x_n represent components or steps. For activity scheduling, these components are either (i) decompositions into temporal activity participations (as is typical in autoregressive formulations); or (ii) decompositions into structured decision sets, such as tour, sub-tour, time, etc (as is typical in compositional formulations).

A key distinction between compositional and autoregressive approaches is that, whereas autoregressive models are trained end-to-end and so are considered generative, compositional models are trained component-by-component. The end-to-end training of autoregressive models effectively decomposes the complex joint distribution into a sequence of simple conditional distributions, allowing explicit modelling of probability density with tractable likelihood maximisation. This general approach is the foundation of generative models used to great success in the image ([Oord et al., 2016](#)) and language ([Brown et al., 2020](#)) domains. However, the component-by-component estimation of compositional models does not allow for explicit modelling of the probability density, making a good estimation of the joint distribution unlikely. Instead, compositional models are typically estimated in isolation and then manually recalibrated to target combined key metrics, such as trip rates. We further note that the decomposition creates biases depending on the (often arbitrary) order of components, and that components are typically substantially simplified, resulting in an inability to generate diverse tour patterns.

Whilst autoregressive approaches address these limitations through end-to-end training, they are not without issues. Important dependencies can be separated by many steps in autoregression. These dependencies must be learnt across multiple steps, requiring significantly more data to train compared to other generative approaches. Given the relative scarcity of activity scheduling data, this is a key barrier to the progress of

autoregressive approaches to activity scheduling and other complex human behavioural modelling tasks. We further note that learning probability density over multiple steps requires assistance, such as teacher forcing (Sutskever et al., 2014), and iterative inference, which is relatively slow.

3.3. Variation Auto-Encoders (VAEs)

We select the VAE (Kingma and Welling, 2013; Rezende et al., 2014) as our preferred generative approach. Distinct from previous compositional approaches, simulation and GANs, VAEs use an explicit generative approach, directly modelling the target distribution as a probability density. Distinct from auto-regressive approaches, which are also explicit generative, VAEs use a structured latent, imposing a simplified prior distribution on the generation process. Combined, these allow for both good *density estimation* and *data efficiency*, both of which are desirable for our schedule generation problem.

More precisely, rather than trying to learn the distribution $p(x)$ directly, a VAE learns $p(x)$ conditional on a latent input z via $p(x|z)$, where z has some prior distribution $p(z)$. This latent structure allows the model to efficiently learn a single mapping from $p(z)$, a compressed and well-defined prior distribution, to an approximation of $p(x)$. VAEs are detailed in Section 4.

3.3.1. Density estimation

Good *density estimation* is the accurate estimation of the probability of all possible activity schedules. Although density estimation is a general requirement of all generative models, in many applications, such as image generation, the generation of individually realistic and feasible samples, such as images of people with the correct number of fingers, is prioritised over the aggregate modelling of the distribution of all possible images. In contrast, density estimation performance is especially important in our context, as we wish to use modelled schedules to represent the choices of real populations, e.g. for transport simulations.

The VAE structured latent prior allows for tractable estimation of likelihood. During training, this results in the model explicitly assigning likelihood to all training data. As discussed by Lucas et al. (2019) and demonstrated by Sajjadi et al. (2018), this generally results in better density estimation than alternative approaches, including GANs. Without access to likelihood estimation, GANs are less biased towards good representation of training data, in extreme cases leading to mode collapse, where a GAN only generates a limited number of common outputs. Previous work by Shone and Hillel (2025) has also demonstrated that VAEs are able to generate schedules that are both representative in aggregate and individually feasible when trained on real-world mobility datasets.

3.3.2. Data and computational efficiency

We define model *data efficiency* as the ability to learn from relatively little data. Compared to many modern generation problems, such as image, video and language modelling, activity schedule data is relatively limited and therefore data efficiency is important. Bond-Taylor et al. (2022) identify VAEs as the most data-efficient generative architecture, and auto-regression as the least. This efficiency stems from the VAE’s structured and compressed latent representation. For this reason, VAEs are often applied in other data-constrained domains, such as tabular data (Apellaniz et al., 2024), 3D

Table 4: Glossary of VAE notation for Section 4

x	schedule
y	labels (conditional data)
z	a latent embedding or representation
$p(x)$	an observed probability distribution of schedules
$p(z)$	the latent prior distribution
$p(\hat{x})$	an estimated probability distribution of schedules
$q_\phi(z x)$	VAE encoder block, also <i>inference</i> process
$p_\theta(x z)$	VAE decoder block, also <i>generative</i> process
$q_\phi(z x, y)$	conditional VAE encoder block, also <i>inference</i> process
$p_\theta(x z, y)$	conditional VAE decoder block, also <i>generative</i> process
\mathcal{L}	loss function
D_{KL}	Kullback-Leibler divergence
\mathcal{I}	mutual information

imaging (Molnár and Tamas, 2024), and medicine (Vazquez et al., 2025). Similarly, VAEs are also often used to augment small data-sets with novel generated samples (Diamantis et al., 2022; Kebaili et al., 2024; Lee et al., 2024).

Good *computational efficiency* is the ability to learn and generate with relatively little time and computational cost. Bond-Taylor et al. (2022) identify VAEs as the most computationally efficient, and auto-regression, diffusion and normalising flows as the least. For diffusion, this is primarily due to the poor efficiency of the generative process, which consists of multiple denoising steps. Conversely, normalising flows reduce the number of steps required for generation, but learning these steps is itself inefficient. Auto-regression is both inefficient during training and generation.

4. Variation Auto-Encoder theory

In this section, we detail the Variational Auto-Encoder (VAE) with a focus on its use as a conditional-generative model. Key notation for this section is summarised in Table 4.

4.1. VAE foundations

VAEs are structured latent generative models that aim to model some distribution $p(x)$ from samples of data x from that distribution. In the following notation we refer to the modelled schedules as \hat{x} and their distribution as $p(\hat{x})$. The *generative process* is modelled as conditional on a random latent variable, $p_\theta(\hat{x} | z)$, which is parameterised by a neural network, called the *decoder*. The latent space z is typically a (multivariate) standard normal, $p(z) = \mathcal{N}(0, I)$. The full generative process then becomes:

$$p(\hat{x}) = p_\theta(\hat{x} | z)p(z), \quad \text{with } p(z) \sim \mathcal{N}(0, I). \quad (2)$$

The intuition behind the VAE is that by learning the mapping p_θ , from the latent prior $p(z)$, to samples from $p(x)$, new samples from $p(x)$ can be generated by randomly sampling from the latent prior and then decoding. To correctly map $p(x)$ across the latent space, and therefore learn inter-sample variation, we additionally learn an *inference process*, $q_\phi(z | x)$, parameterised by a neural network called the *encoder*.

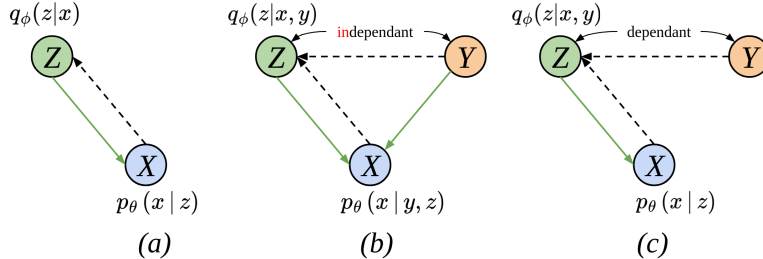


Figure 1: Graphical models of generative (green) and inference (dashed) processes. (a) VAE, (b) CVAE with independent latent space, and (c) CVAE with dependent latent space, i.e. with latent space entangled with labels.

To work successfully, a VAE must be able to both reconstruct samples from the latent representation using its generative process, $p_\theta(\hat{x} | z)$, i.e the decoder, and distribute the latent space as per the prior $p(z)$ using its inference process, $q_\phi(z | x)$, i.e the encoder.

The combined processes, $p_\theta(\hat{x} | z)q_\phi(z | x)$, is trained end-to-end to minimise reconstruction loss, typically the cross entropy between input x and output \hat{x} . The inference process q_ϕ is additionally trained to minimise divergence between the latent $z = p_\phi(x)$ and the target prior distribution $p(z)$, typically achieved using Kullback-Leibler Divergence (D_{KL}).

More formally, VAEs optimise a variational lower bound known as the Evidence Lower Bound (ELBO), resulting in the following loss function:

$$\mathcal{L}_{\text{vae}}(\theta, \phi) = \mathbb{E}_{q_\phi(z|x)} [\log p_\theta(\hat{x} | z)] - D_{KL}(q_\phi(z | x) \| p(z)). \quad (3)$$

In the above equation, the first term is referred to as the *reconstruction* loss and the second as the *regularisation* loss or D_{KL} or latent divergence.

The latent space in the VAE acts as a compressed representation of $p(x)$, and the prior defines its distribution. Unlike the auto-regressive formulation from Equation 1, this maps full schedules (and their intra-dependencies) to single latent representations. This imposes some restrictions on model expressiveness but makes training relatively data-efficient and generation computationally efficient. A reasonable intuition for the VAE is that it *interpolates* real observations by first learning a mapping to a structured latent (with a compressed, well-defined, and continuous distribution), so that it can *interpolate* across this instead.

4.2. Latent disentangling (β VAE)

The D_{KL} component of the VAE loss can be considered as regularising the reconstruction process. By encouraging the latent space to conform to the prior, this regularisation limits or at least structures how information is passed through the latent bottleneck, impacting reconstruction. During training, if the regularisation is too low, then the inference process will poorly comply with the prior. The resulting difference between $p_\phi(z)$ and the prior $p(z)$ causes poor performance when generating new samples. Conversely, if the regularisation is too high, the combined inference and generation processes ($p_\theta(\hat{x} | z)q_\phi(z | x)$) will fail to reconstruct samples, also resulting in poor performance when generating new samples. The balance between reconstruction and regularisation is

dependent on model architecture, but typically tuned within the loss function using the hyperparameter β as follows:

$$\mathcal{L}_{\beta\text{vae}}(\theta, \phi) = \mathbb{E}_{q_{\phi}(z|x)} [\log p_{\theta}(\hat{x} | z)] - \beta D_{\text{KL}}(q_{\phi}(z | x) \| p(z)). \quad (4)$$

As per β VAE (Higgins et al., 2016) the regularisation from D_{KL} can also be considered as *disentangling* (Burgess et al., 2018) the latent space. By increasing β , the VAE is encouraged to more efficiently use the latent space, specifically to arrange uncorrelated generative information into separate latent dimensions.

4.3. Conditionality in VAEs

Conditional VAEs (CVAEs) (Kingma et al., 2014) extend the VAE framework to learn a conditional distribution $p(x | y)$, where y are labels that can be used to control the final generation process. The decoder architecture and, therefore, generative process, is extended to encompass this conditionality as $p_{\theta}(\hat{x} | y, z)$. Similarly, the encoder architecture and, therefore, inference process, is extended as $q_{\phi}(z | y, x)$. This new formulation is shown in Figure 1(b). After successful training, new samples from $p(\hat{x} | y)$ can be generated by passing the target labels and new random samples from $p(z)$ through the decoder:

$$p(x | y) = p_{\theta}(\hat{x} | y, z)p(z), \quad \text{with } p(z) \sim \mathcal{N}(0, I). \quad (5)$$

By assuming that z and y are independent, i.e. $p(z, y) = p(z)p(y)$ we can formulate the following CVAE loss function:

$$\mathcal{L}_{\text{cvae}}(\theta, \phi) = \mathbb{E}_{q_{\phi}(z|x,y)} [\log p_{\theta}(\hat{x} | y, z)] - \beta D_{\text{KL}}(q_{\phi}(z | x, y) \| p(z)). \quad (6)$$

This is broadly unchanged from the previous β VAE loss function in Equation 4. However, the assumption of independence between z and y is important. It is useful to consider each schedule as having a representation that can be decomposed into known latent (labels) and random latent (z) representations. For controllable generation, i.e. where new samples can be generated for specific labels, the known latents and random latents need to be independent. If z and y are dependent, then the generative process requires knowing $p(z | y)$:

$$p(\hat{x} | y) = p_{\theta}(\hat{x} | y, z)p(z | y). \quad (7)$$

Label controllable generation is then no longer possible by randomly sampling from the prior $p(z)$. This failure mechanism is illustrated in Figure 1(c).

It is not possible to trivially remove dependence between the latent and labels by removing the conditionality of z on labels, because x is also conditional on labels, giving us the equivalent $p_{\phi}(z | p(x | y))$. Counter-intuitively, labels are included in encoder architectures so that the encoder can explicitly learn what to ignore in its latent encoding of x .

As per the β VAE in Section 4.2, D_{KL} is used to regularise or bottleneck information through the latent layer, such that the model is encouraged to reduce or remove label information, which is more efficiently available to the generation process as input labels. We can therefore extend the idea of *disentangling* a VAEs latent space (as per Section 4.2), to *disentangling* a CVAEs combined latent space and input labels.

Table 5: Summary of methodology Section 5

Section 5.1	Informal problem definition
Section 5.2	Experiment overview
Section 5.3	Activity schedule definition
Section 5.4	Labels definition
Section 5.5	Real sample definition
Section 5.6	Target labels definition
Section 5.7	Data

4.4. Latest research into CVAEs

CVAE untangling of label information from conditional information using β is fundamentally limited because β also regularises the passing of schedule information through the latent representation. This is shown formally in [Appendix A](#). This makes the development of VAEs with good conditional capability challenging. Existing work on this disentanglement challenge ([Larsen et al., 2016](#); [Mescheder et al., 2017](#); [Chen et al., 2016](#)) radically modify the VAE approach, introducing auxiliary models and/or adversarial training. Such models can be considered as VAE-GAN composites, improving conditional capability, but at the expense of density estimation and data efficiency, both critical in our case.

The Vector-Quantised VAE (VQVAE) ([van den Oord et al., 2017](#)) has demonstrated excellent conditional generation for text-to-image and text-to-video tasks ([Tang et al., 2022](#)). However, VQVAE does not impose a prior latent distribution as per a regular VAE; instead, an auxiliary prior model has to be separately learnt to model the latent distribution. This approach can be broadly considered as compression, then generative modelling of this compression. Alternative priors and regularisations have also been proposed, most notably the sliced Wasserstein Auto-encoder (SWAE) ([Kolouri et al., 2019](#)). We formally compare the regular VAE to a VQVAE, a SWAE, and a simple uniform categorical latent embedding (CatVAE) ([Jang et al., 2016](#)) in [Section 6.11](#).

We introduce ActVAE, a CVAE-based generative model with conditional capability for modelling activity schedules. Our key contribution is to incorporate conditionality into a VAE architecture with good generative capability, allowing it to be used in existing transport demand modelling frameworks.

5. Methodology

The contents of the methodology section are summarised in [Table 5](#).

5.1. Informal problem definition

We consider a sample of individuals, each associated with a set of labels (y), such as household size, car ownership, and socio-demographic attributes, as well as a recorded activity schedule (x). We consider this sample to be drawn from the population, so that it is representative of the conditional distribution of schedules on labels. This data is typically sampled from a real population through a structured travel survey. We aim to model the population probability density of activity schedules, conditional on labels, using this sample, such that the model can then generate new schedules for new samples of input labels.

Table 6: summary of experiment model generative and conditional capabilities

Model Name	Explicit generative	Conditional	
ConditionalRNN	-	✓	Based on Koushik et al. (2023)
GenerativeRNN	✓	-	Shone and Hillel (2025)
ActVAE	✓	✓	this paper

By modelling the distribution of schedules conditional on labels, we are able to generate schedules dependent on input labels. For example, we can generate a schedule for an individual with a specific set of socio-economic characteristics (potentially previously unobserved). This model can then be used to predict a new distribution of activity schedules for a target distribution of labels. This model is then applicable for (i) diverse upsampling, including de-biasing, of activity schedule data, and (ii) predicting new activity scheduling behaviour, such as due to demographic shifts or infrastructure and policy interventions.

Note that labels do not need to be restricted to socio-economic attributes, but can also include other information potentially relevant to the schedule generation processes discussed in Section 1, such as accessibility or weather conditions. Key notation for this section is summarised in Table 7.

5.2. Experiment Overview

We train our conditional-generative model, ActVAE, to model activity schedules from the UK National Travel Survey (NTS) (Section 5.7) and evaluate the resulting model for conditional and generative capabilities as described in Section 6.13. We provide evidence to support the final model architecture with supplementary experiments using alternative generative models in Section 6.11 and an ablation study in Section 6.12.

ActVAE combines both conditional and explicit generative processes to generate schedules. The conditional process of ActVAE is analogous to traditional conditional approaches, where variation is modelled depending on input information only. In contrast, the explicit generative process of ActVAE directly tries to model the distribution of schedules as a density distribution. We consider the importance of these processes by comparing ActVAE to two baselines: a model with an explicit generative process only (no conditionality), and a model with a conditional process only (no explicit generative process). Specifically, we compare to (i) ConditionalRNN - a purely *conditional* model that outputs the most likely schedule given the input labels, based on [Koushik et al. \(2023\)](#), and (ii) GenerativeRNN - a purely *explicit generative* VAE without conditional capability as per [Shone and Hillel \(2025\)](#).

Model capabilities (explicit generative versus conditional) are summarised in Table 6 and illustrated in Figure 2. All models use the same basic schedule and label encodings, encoder and decoder architectures and loss functions to make comparisons fairer.

5.3. Activity Schedule Definition

We define a single activity schedule x as an ordered sequence of activity types a_n with associated durations d_n , summing to T . As per Section 6.1 travel durations are considered part of activity durations, such that each schedule is composed only of activities. The length L_x of the sequence may vary per schedule, but note we later impose a limit as per

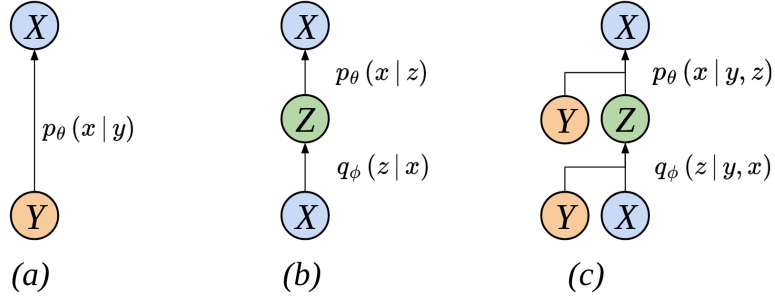


Figure 2: Model generative and conditional processed (a) ConditionalRNN (conditional), (b) GenerativeRNN (explicit generative), and (c) ActVAE (conditional-generative).

Table 7: Glossary of notation for problem definition in Section 5

x	schedule
a_n	activity type, indexed in schedule sequence by n
d_n	activity duration, indexed in schedule sequence by n
L_x	schedule sequence length
T	schedules total duration
y	labels composed of multiple variables y_1, y_2, \dots, y_{N_L}
N_L	the total number of label variables
$p(x, y)$	the supposed <i>real</i> joint distribution of schedules and labels
$p(\hat{x}, y)$	the estimated <i>real</i> joint distribution of schedules and labels
S_{real}	sample of labels from the <i>real</i> distribution with corresponding schedules
S_{target}	an abstract sample of labels from some <i>target</i> distribution of labels $p(y')$
S_{eval}	labels from S_{real} , used for generative evaluation

Section 6.1. We choose a total duration of 24 hours, starting and ending at midnight, for our experiments:

$$x = [(a_1, d_1), (a_2, d_2), \dots, (a_{L_x}, d_{L_x})], \quad \text{where} \quad \sum_{n=1}^{L_s} d_n = T. \quad (8)$$

5.4. Labels definition

We define each schedule as having some associated conditional information, which we refer to as labels y . Labels are composed of N_L variables, such as income, gender and so on:

$$y = [y_1, y_2, \dots, y_{N_L}]. \quad (9)$$

For simplicity, we represent all variables as nominal tokens, where each token represents membership to a specific category for each label, but future work may wish to experiment with scalar encodings of some variables.

We use labels as a general term to describe any input information that can be used by a model to predict an output schedule. Labels can be composed of any information related to a schedule, such as the day of the week or weather conditions at the time the schedule occurred, or related to the individual who undertakes the schedule, such as their age, income, or whether they own a car.

5.5. Real Sample Definition

We consider a sample of pairs of schedules $x \in \mathcal{X}$, where \mathcal{X} is the space of all possible schedules, and labels $y \in \mathcal{Y}$, where \mathcal{Y} is the space of all possible labels. These pairs of schedules and labels are drawn from a target joint distribution of schedules and labels $p(x, y)$, such that we consider our sample to have the same joint distribution as the target, which we refer to as the *real distribution*. This distribution describes realised human activity schedules, encompassing both individual preferences and environmental constraints such as accessibility and congestion.

Let the *real sample* be a finite dataset of N_{real} observed schedules and labels:

$$\mathcal{S}_{real} = [(x_1, y_1), (x_2, y_2), \dots, (x_{N_{real}}, y_{N_{real}})] \subset \mathcal{X}, \mathcal{Y}, \quad \text{with} \quad (x, y) \sim p(x, y). \quad (10)$$

For training and reporting of validation and test losses, we use an 80%-10%-10% split of the real sample.

5.6. Target labels definition

For modelling or generating new samples of synthetic schedules, we define a target set of labels:

$$\mathcal{S}_{target} = \{y_1, y_2, \dots, y_{N_{target}}\} \subset \mathcal{Y}, \quad \text{with} \quad y \sim p'(y). \quad (11)$$

Note that these labels can have a novel distribution $p'(y)$ and a variable number of samples N_{target} . This distribution can be used to represent a change, such as an aged population or better accessibility, that is expected to affect the distribution of schedules.

Table 8: Summary of labels used for experiments

Label	Categories
Gender	{male, female, unknown}
Age	{0-4, 5-10, 11-15, 16-19, 20-29, 30-39, 40-49, 50-69, 70+}
Car Access	{yes, no, unknown}
Work Status	{employed, education, unemployed}
Income (household)	{highest, high, medium, low, lowest}

For our experiments, we use labels from the real sample as the target:

$$\mathcal{S}_{\text{eval}} = \{y_1, y_2, \dots, y_{N_{\text{real}}}\} \subset \mathcal{Y}, \quad \text{with } y \sim p(y). \quad (12)$$

This allows comparison with the evaluation of the purely generative GenerativeRNN model, which does not condition on labels

5.7. Data

For the real sample of schedules and labels, we extract 59,265 24-hour trip diaries from the 2023 UK National Travel Survey (NTS) trips table². Corresponding labels for the real sample are extracted from NTS household and individual data tables. We extract the following labels: gender, age, car access, work status, and household income. The choice of labels is designed to reflect likely requirements of a transport demand modelling framework. The influence of additional labels is explored in [Appendix F.3](#). Label categories are summarised in [Table 8](#).

The NTS trip data is converted into schedules using PAM ([Shone et al., 2024](#)). This process includes: (i) removing trips, and (ii) simplifying activity types to the set home, work, education, medical, escort, other, visit, and shop (8 types total). To remove trips, we extend the prior activity durations to include the following trip duration, such that activity start times are maintained. [Figure 3](#) shows example extracted and processed activity sequences.

As per previous work by [Shone and Hillel \(2025\)](#), two types of infeasibility (structural-zeros) are defined: (i) non-home-based infeasibility - not starting and/or ending at home, and (ii) consecutive activity infeasibility - two or more home, work or education activities happening consecutively. To establish this feasibility in the training set, we filter to exclude non-home-based schedules and consecutive home, work and education activities are combined into a single activity.

The resulting schedules and labels are then considered as the real sample $\mathcal{S}_{\text{real}}$ and the evaluation sample $\mathcal{S}_{\text{eval}}$, used for generative evaluations. We use an 80% sample of this data for training, 10% for validation, and 10% for reporting test losses.

6. Model Design

In this section, we describe the design and operation of ActVAE. We also define two baseline models: GenerativeRNN and ConditionalRNN. The baseline *explicit generative*

²<https://ukdataservice.ac.uk>

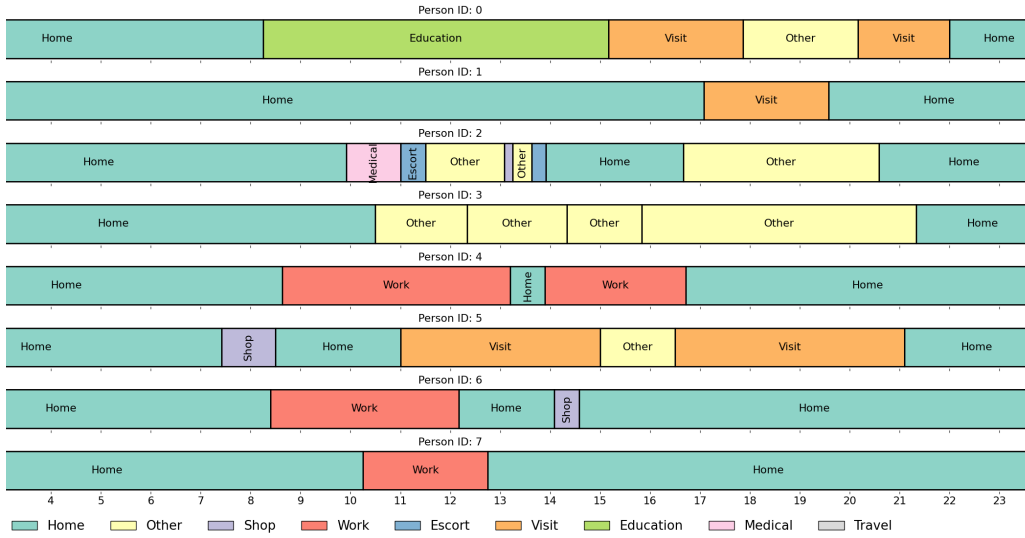


Figure 3: Example UK NTS Schedules

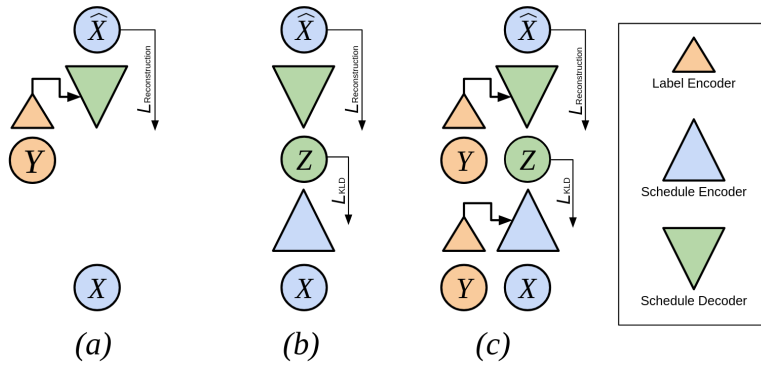


Figure 4: Summary of model encoder and decoder architectures and loss functions (a) ConditionalRNN (conditional), (b) GenerativeRNN (explicit generative), and (c) ActVAE (conditional-generative).

Table 9: Summary of components used by models

Component	Section	ConditionalRNN	GenerativeRNN	ActVAE
Continuous schedule encoding	6.1	✓	✓	✓
Reconstruction loss	6.2	✓	✓	✓
Latent KLD loss	-	-	✓	✓
Schedule encoder	6.3	-	✓	✓
Schedule decoder	6.4	✓	✓	✓
Conditionality injection	6.5	✓	-	✓
Continuous embedding block	6.6	✓	✓	✓
Continuous unembedding block	6.7	✓	✓	✓
Labels embedding block	6.8	✓	-	✓
Latent block	6.9	-	✓	✓

Table 10: Glossary of model design notation in Section 6

L	maximum embedded schedule sequence length (16)
\mathcal{A}	schedule embedding tokens
N_a	number of embedding tokens
N	encoder/decoder block depth (number of layers)
S	schedule embedding hidden size
H	label embedding hidden size
α	loss function duration component weight
α	loss function regularisation component weight
LSTM	Long Short-term memory (Hochreiter and Schmidhuber, 1997)
l	individual label belonging to labels y
Y	set of individual labels composing y
c	category of label l belonging to set \mathcal{C}_1
N_c	number of schedules in sample of category c
N_l	number of schedules in sample of category c
\mathcal{D}_c	category-level joint density evaluation metric
\mathcal{D}_l	label-level joint density evaluation metric
$\mathcal{D}_{\text{joint}}$	domain-level joint density evaluation metric

model, GenerativeRNN, is a non-conditional VAE detailed by Shone and Hillel (2025) (specifically the ContRNN architecture). The baseline *conditional* model, ConditionalRNN, is based on models by Koushik et al. (2023), but modified to use a continuous schedule encoding, described by Shone and Hillel (2025). This modification improves on the original performance and makes all model designs more consistent as illustrated in Figure 4.

All models use a Recurrent Neural Network (RNN) architecture and share model components as per Table 9. These components are detailed in the following sections. Model designs are selected based on previous work and optimised using experimentation detailed in Sections 6.11 and 6.12. Consistency of design additionally allows for fairer comparisons of model capabilities. Model training and hyper-parameteres are detailed in Section 6.10. Key notation for this section is summarised in Table 10.

6.1. Continuous schedule encoding

The models all use a continuous schedule encoding, where schedules are encoded as sequences of discretely encoded activity types with continuously encoded durations (between zero and one days). This encoding provides a compact and natural representation

of schedules and has been shown to outperform the alternative discrete encoding (Shone and Hillel, 2025). Similar to language models, sequences start with a special *start of sequence* token and are padded as required with *end-of-sequence* tokens, all of zero duration, up to a maximum total sequence length (L) of 16. We refer to the combined set of activity tokens (including start and end of sequence padding token) as \mathcal{A} of size N_a .

6.2. Continuous reconstruction loss

The continuous schedule encoding requires a combined reconstruction loss to incorporate both the discrete representation of activity types and the continuous representation of activity durations. We use categorical cross-entropy for the activity type component of reconstruction loss. Cross-entropy is calculated between activity prediction $p(a)$ and the one-hot encoded ground truth $q(a)$, for each token in $a \in \mathcal{A}$, at each step of the schedule encoding n . These are then averaged across all L steps.

For the durations component of the reconstruction loss, we use the mean squared error between the predicted duration \hat{d} and ground truth duration d , for each schedule step n . We introduce an additional hyperparameter α , detailed in Table 11, to weight the duration loss component.

$$\mathcal{L} = -\frac{1}{L} \sum_{n=1}^L \sum_{a \in \mathcal{A}} p(a_n) \log q(a_n) + \frac{\alpha}{L} \sum_{n=1}^L (d_n - \hat{d}_n)^2 + \beta D_{\text{KL}}. \quad (13)$$

We additionally employ masking and weighting of the loss function. Firstly, for each sequence, losses are masked to exclude all but the first predicted *end-of-sequence* tokens. This prevents the model from benefiting from the correct prediction of padding tokens. Losses for each sequence are then weighted by the inverse frequency of their labels. Weights are normalised by batch to average one. This weighting biases the model towards schedules with less common label combinations.

6.3. Schedule encoder

The ActVAE architecture (Figure 5) is composed of an encoder block and a decoder block. As per Section 4.3, the encoder parametrises the inference process $p_\phi(z | x, y)$, the decoder the generation process $p_\theta(x | z, y)$. We use a latent block detailed in Section 6.9 to parametrise the prior $p(z)$.

The encoder block iteratively progresses through each step of the input sequences, first embedding input activity type and duration into a size S hidden vector as per Section 6.6, then passing into N stacked LSTM units of size S . The LSTM units pass a learnt hidden state from step to step. The output hidden state from the final unit is flattened and passed via a feed-forward block, with output size S , to the latent block.

6.4. Schedule decoder

The decoder block is similarly based around N stacked LSTM units of size S . The size S and depth N control the complexity or capacity of the hidden states of the encoder and decoder blocks. The output from the latent block is first resized using a feed-forward block and reshaped into the hidden state of the first decoding LSTM unit. This first unit uses a start-of-sequence token as input, further steps then use the argmax sampled output from the previous step. During training, we use 50% teacher forcing, where previous

predictions are replaced by training data, to improve training stability. Input sequence steps are embedded as per the encoder. LSTM unit outputs are un-embedded from size S vectors into predicted activity types and durations using un-embedding blocks as per Section 6.7.

6.5. Conditionality injection

To provide label context for conditionality, labels are first encoded using a label encoder block (Section 6.8) to output a hidden vector of size H . Similarly to the size S , H controls the complexity or capacity of the hidden state of the label encoder block. This vector representation of labels is then input to the encoder and or decoder block, as per Figure 5 for ActVAE. For the encoder block, the label vector is resized via a linear layer and input to the initial LSTM unit hidden state. The decoder block operates similarly, but first uses addition to combine the label and latent vectors. Note that in both cases the label representation of size H is first resized via linear layers to equal the block hidden state input size ($2 \times N \times S$).

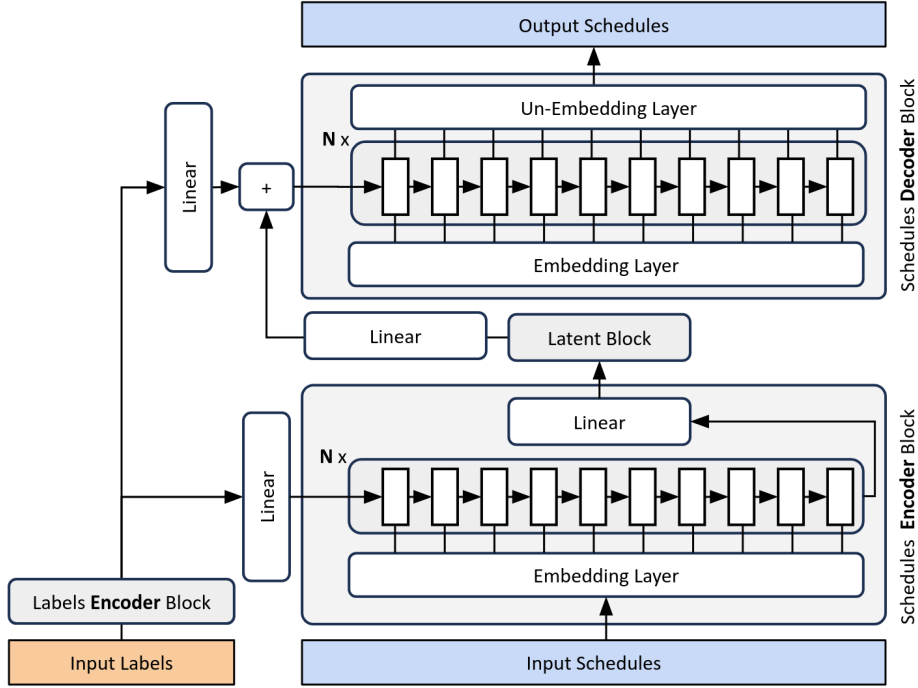


Figure 5: ActVAE architecture

6.6. Embedding Block

The continuous schedule encoding combines a discrete activity type encoding and continuous duration encoding. This encoding is embedded into a vector of size S using a custom *continuous embedding layer*. Input activity types and durations are first split, and then tokens are transformed into vectors of size $S - 1$ using a learnt embedding

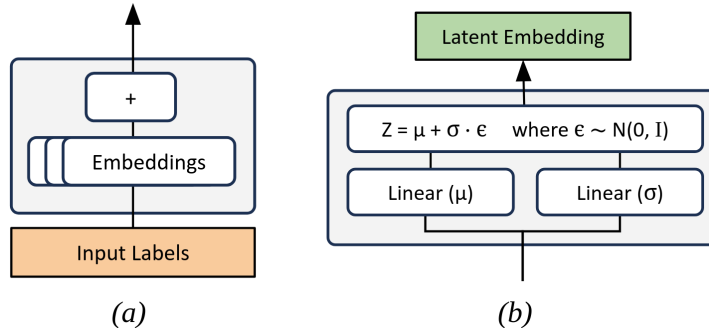


Figure 6: (a) Label encoder block, and (b) latent block

layer. The resulting activity embedding vectors are then concatenated back with their durations. Note that activity types also include the special start and end of sequence tokens.

6.7. Un-Embedding Block

At each step the model LSTM blocks output vectors of size S . These are un-embedded into activity type probabilities and durations using a custom *continuous un-embedding layer*. Output vectors are first resized using a fully connected linear layer, which outputs vectors of size $N_a + 1$ (number of token types, including special start and end of sequence tokens, plus a duration scalar). Each duration is passed through a sigmoid activation so that all duration values are between zero and one. The remaining activity type vectors are decoded into probabilities using a soft-max layer.

Completed sequence durations are then normalised by the total duration of each predicted sequence. This normalisation enforces the intended duration T . Note that the calculation of total predicted duration excludes any durations *after* the first end of sequence token.

For generation, we sample from activity type probabilities using argmax. Activities and their durations for each sequence are then concatenated back together. Argmax sampling removes stochasticity from the architecture, forcing all variance to be modelled by the VAE generative process.

6.8. Label Encoder Block

The label encoder block in Figure 6(a) is used to embed multiple categorical labels as a vector of size H . The label encoder block first individually encodes each categorical label using learnt embeddings of size H . The resulting vectors are combined through addition.

6.9. Latent Block

Figure 6(b) presents the latent block design used by the generative models. Within the block, the latent layer, a vector of length six, is sampled from a normal distribution with mean μ and standard deviation σ . This is commonly referred to as the *reparametrisation trick*. Both μ and σ are both vectors with the same size as the latent layer. μ and σ are resized from the encoder output using fully connected linear layers.

Table 11: Model hyperparameters

Model	RNN Block Size (N.S.H)	Latent Size	Learning Rate	Batch Size	β	α	Drop Out
ActVAE	4.256.64	6	0.001	1024	0.01	200	-
ConditionalRNN	4.128.32	-	0.001	1024	-	200	0.1
GenerativeRNN	4.256.-	6	0.001	1024	0.01	200	0.1

6.10. Model Training and Hyper-parameters

We train models until validation loss stabilises, typically for around 100 epochs. We use Adam for gradient descent. Model training hyperparameters are reported in Table 11. The latent size, α and β are selected via an extensive grid search. The remaining hyperparameters are chosen to optimise validation loss using the Tree-structured Parzen Estimator by Optuna (Akiba et al., 2019).

6.11. Alternative generative approaches

We compare the standard VAE to three alternative latent generative models; (i) Categorical latent embedding (CatVAE) with Gumbel-Softmax as per Jang et al. (2016), (ii) Vector-Quantised VAE (VQVAE) by van den Oord et al. (2017) - a categorical latent embedding using token embeddings, and (iii) Sliced Wasserstein Auto-Encoder (SWAE) by Kolouri et al. (2019).

These models and their evaluation are detailed in Appendix B. The VQVAE approach is particularly powerful, both using a large tokenised latent embedding and the flexibility of a learnt prior. The VQVAE is the core approach in many modern generative architectures, such as text-to-image generation (Tang et al., 2022). However, we find that categorical embeddings do not work well, likely because of the continuous nature of schedule durations and the relatively small data availability, making it challenging to learn a good prior for the VQVAE. As per the regular VAE, SWAE employs a continuous latent representation with a normal prior, but utilises a more flexible regularisation of the prior using Wasserstein distance, potentially enabling better generation. We find that SWAE evaluations are relatively comparable, but generally still worse than the regular VAE and therefore the standard VAE approach of continuous latent embedding, normal prior, and KLD regularisation is preferred.

6.12. Alternative model architectures

Our schedule encoder and decoder are based on a recurrent architecture using LSTM units. Shone and Hillel (2025) demonstrate that this recurrent architecture performs better than alternative fully-connected and convolutional approaches. We contribute conditional capability to this architecture through the *injection* of conditional label information via a label encoder block. We explore many ways of *injecting* this conditionality and find that it is possible to bias the model either towards conditional capability or generative capability.

Models can be biased towards *conditional* capability by (i) increasing the size of the label embedding, (ii) *injecting* the label embedding at every step of un-embedding layers,

and (iii) using concatenation for *injection* of label embeddings. These improve conditional capability but at the expense of generative capability. Conversely, models can be biased towards *generative* capability by (i) increasing the size of the latent embedding, (ii) *injecting* the label embedding at fewer locations, and (iii) using addition for *injection* of label embeddings. These improve generative capability but at the expense of conditional capability.

The final ActVAE architecture provides an optimal balance between conditional and generative capability based on an extensive grid search of (i) loss weightings, (ii) block depths and hidden sizes, (iii) omission versus addition versus concatenation of label information at encoder and decoder hidden layers, and (iv) omission versus addition versus concatenation of label information at encoder and decoder embedding and unembedding layers. A selection of these experiments are summarised as an ablation study in [Appendix C](#).

6.13. Evaluation methodologies

In our results section, we evaluate model performance using a broad range of approaches, summarised in [Table 12](#). Of these, joint density estimation is novel and likely the most important, as it evaluates how well models can learn the joint distribution of schedules and labels $p(x, y)$. The methodology for joint density estimation is detailed in [Section 6.14](#).

Most of our evaluations consider the generative process of the model (as it would be used in an application). In these cases, after training, a *synthetic sample* of schedules is generated, conditioned on target labels $\mathcal{S}_{\text{eval}}$ as per [Section 5.6](#). We refer to the distribution of these schedules as $\hat{p}(x)$ and the joint distribution of schedules and their labels as $\hat{p}(x, y)$. Note that we have defined $\mathcal{S}_{\text{eval}}$ as equal to labels from $\mathcal{S}_{\text{real}}$ so that the GenerativeRNN model, which does not have a conditional capability, can still be compared for joint density estimation evaluation.

6.14. Density estimation and joint density estimation

Density estimation considers the closeness of the synthetic distribution of schedules $\hat{p}(x)$ to the real distribution $p(x)$. Density estimation for high-dimensional data is non-trivial. As per [Shone and Hillel \(2025\)](#), we approximate density estimation using earth-movers distances for a broad range of marginal and conditional distributions. For high-level evaluation, these distances are aggregated into the *domain-level* metrics; participations, transitions, and timings. In all cases, lower distances are better, suggesting a closer match between the distribution of real and synthetic schedules.

Existing density evaluation considers the distribution of synthetic schedules $\hat{p}(x)$. We extend this for our generative-conditional case to consider the joint distribution of synthetic schedules and their labels $\hat{p}(x, y)$. For convenience, we define a general density evaluation distance D_* as a function F of real and synthetic samples of schedules:

$$D_* = F(\mathcal{S}_*, \hat{\mathcal{S}}_*) \tag{14}$$

The density estimation of the joint distribution of schedules and labels is approximated by further conditioning on label categories. For example, we can consider the distribution of a sample of schedules conditioned on the *employed* work status, informally, as follows:

$$\mathcal{S}_{\text{employed}} = \{x_1, x_2, \dots, x_{N_{\text{employed}}}\}, \quad x \sim p(x \mid \text{employed}) \quad (15)$$

This sample is extracted from the real and synthetic samples and used to evaluate density estimation distances conditioned on the *employed* work status:

$$D_{\text{employed}} = F(\mathcal{S}_{\text{employed}}, \hat{\mathcal{S}}_{\text{employed}}). \quad (16)$$

This is then repeated for each other work status category (unemployed and in education) and for all other label categories as per Table 8. The resulting distances are then averaged, weighted by the size of each sample.

Formally, we consider the combined set of labels $y \in \mathcal{Y}$ as decomposed into individual labels $l \in Y$, where $Y = \{\text{gender, age, income, work status, car access}\}$. Each label then has categories $c \in \mathcal{C}_l$, where \mathcal{C}_l is the possible set of categories for each label l .

We then define category-level density evaluation as;

$$D_c = F(\mathcal{S}_c, \hat{\mathcal{S}}_c), \quad (17)$$

label-level joint density evaluation as;

$$D_l = \sum_{c \in \mathcal{C}_l} \frac{N_c}{N_{\text{eval}}} D_c, \quad (18)$$

and domain-level joint density evaluation as:

$$D_{\text{joint}} = \sum_{l \in L} \frac{1}{|L|} D_l. \quad (19)$$

This approach to joint density estimation is limited to *marginal* label distributions only. Similarly to the schedule density estimation approach, this prevents consideration of more complex distributions, but by considering all *first-order* label marginals, schedule marginals, and conditionals, a reasonable approximation of the quality of the full joint distribution can be expected.

7. Results

Figures 7 and 8 illustrate the high-level capabilities of models by comparing the distributions of activity *sequences* (the ordering of activity participations) and *frequencies* (when activity participations occur) by employment type (employed, student, or unemployed). In each case, distributions are compared to the target real distribution. The ConditionalRNN approximates the most likely sequence and timing of activities for each employment class, but without generative capability, fails to generate a realistic distribution of either sequences or frequencies. The GenerativeRNN instead generates a realistic overall distribution of sequences and frequencies, but without a conditional capability, it cannot model differences between the employment classes. ActVAE combines both generative and conditional capability, so it can model distributions for each class most similar to the real target distributions.

Neither the GenerativeRNN nor ActVAE exactly match the target distributions. For example, ActVAE generates too few *education* activities and too many *other* activities for

Table 12: Evaluation methodologies summary

Evaluation	Ref.	Description
Reconstruction losses	Section 7.1	Validation and test set reconstruction losses.
Conditionality	Section 7.2	Qualitative evaluation of expected label responses.
Feasibility	Section 7.3	Schedule feasibilities as per Shone and Hillel (2025).
Creativity	Section 7.3	Model creativity as per Shone and Hillel (2025).
Joint density estimation		Methodology detailed in Section 6.14
Domain-level	Section 7.4	Domain-level density evaluation.
Label-level	Section 7.5	Label-level density evaluations.
Category-level	Section 7.6	Selected category-level density evaluations.
Latent entanglement	Section 7.7	Evaluation of latent-label disentangling.
Model performance	Section 7.8	Train and generation run times.
Supplementary studies		
Forecasting scenario	Appendix F.1	Forecasting demonstration.
Data availability	Appendix F.2	Sensitivity to data availability.
Label availability	Appendix F.3	Sensitivity to label availability.
Foundational model	Appendix F.4	Learning a foundational model.

students. The bi-modality of timings for unemployed persons is also not well modelled. Both the generative and conditional capabilities of the models are quantified and detailed in the following results sections, summarised in Table 12. We supplement results detailing selected joint distributions in Appendix E, and with various case studies in Appendix F.

7.1. Reconstruction losses

We first evaluate model reconstruction losses using withheld test data from $\mathcal{S}_{\text{real}}$. This considers the ability of the model reconstruction process to generalise and allows us to monitor over-fitting. We consider both the mean Negative Log Likelihood (NLL) of activity predictions and the Mean Squared Error (MSE) of duration predictions. Table 13 presents train and test set losses. Train and test set losses are comparable for all models, indicating they are not over-fitting.

The ConditionalRNN model constructs schedules based on input labels only. The GenerativeRNN model, in contrast, does not use label information and must pass all information for reconstruction through a latent representation. Both models perform similarly for activity prediction, but the label-only ConditionalRNN performs worse for duration prediction. This suggests that duration information is more efficiently embedded as a random distribution, likely because variance in activity *durations* is not well explained using labels relative to activity *types*. For example, we can reason that participation in a *work* activity is reasonably conditional on the *employment* label, but that there is no such clear condition for the duration of the activity.

Whereas the baseline models maximise reconstruction using label information (for the ConditionalRNN) and random latents (for the GenerativeRNN), ActVAE, by combining both label and random latent information, outperforms both baseline models at both activity type and duration reconstruction. This shows that the conditional information, passed by labels, and random information, passed by latents, are both of importance for modelling schedules, and are to some extent orthogonal. In other words, this suggests that the random variation of schedules, i.e. variation that is not explainable by labels,

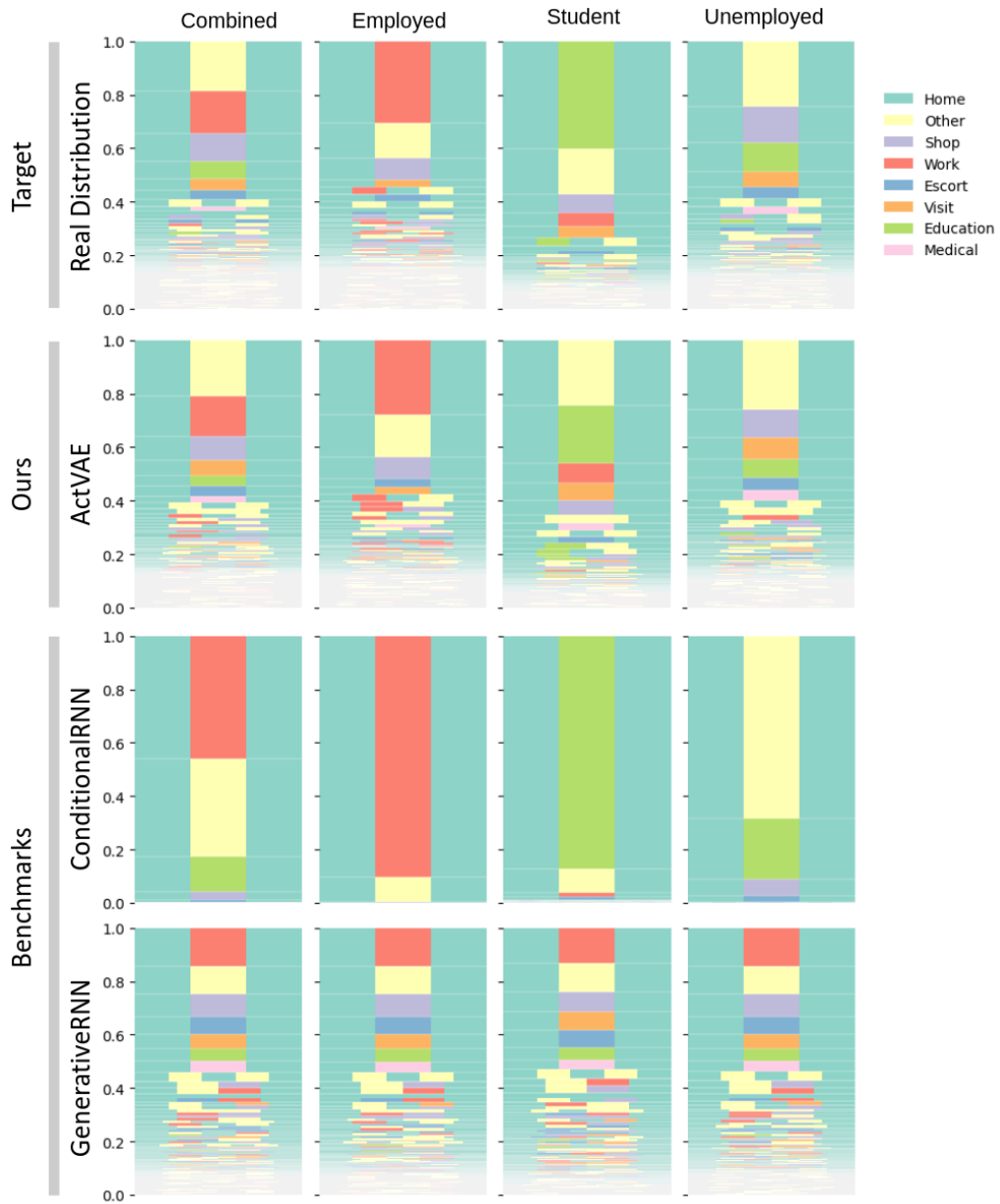


Figure 7: Summary of activity sequence distributions, combined and by employment class, for (i) the real or target distribution, (ii) ActVAE, (iii) the conditional only ConditionalRNN, and (iv) the generative only GenerativeRNN.

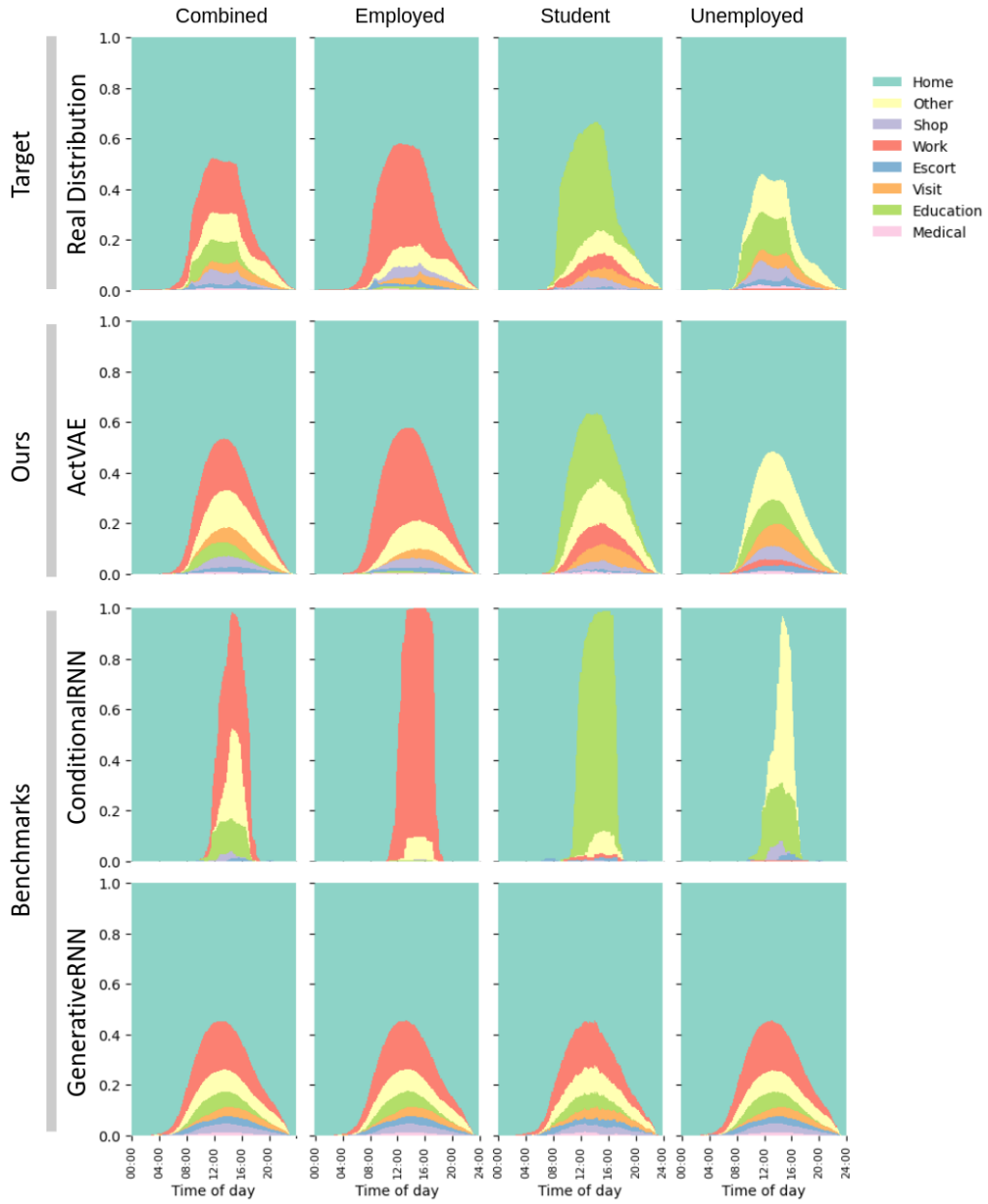


Figure 8: Summary of activity frequency distributions, combined and by employment class, for (i) the real or target distribution, (ii) ActVAE, (iii) the conditional only ConditionalRNN, and (iv) the generative only GenerativeRNN.

Table 13: Reconstruction losses

	ConditionalRNN		GenerativeRNN		ActVAE	
	mean*	var.	mean*	var.	mean*	var.
Training Set Losses						
Duration Loss (MSE)	0.00128	0.00000	0.00054	0.00000	0.00014	0.00000
Activity Loss (NLL)	0.04809	0.00000	0.06100	0.00047	0.02321	0.00000
Test Set Losses						
Duration Loss (MSE)	0.00129	0.00000	0.00054	0.00000	0.00022	0.00000
Activity Loss (NLL)	0.04825	0.00000	0.06216	0.00050	0.02374	0.00000

* mean loss from 5 model runs

is relatively significant. More simply, we note that a large amount of schedule variance *is not* explained using labels alone. We know, for example, that a person with the same labels will have different schedules on different days. However, it is not clear, before this work, the importance of modelling this random variance. The following sections provide evidence of the importance of modelling random variation using both density and mutual information estimation.

7.2. Conditional evaluation

The consideration of reconstruction losses evaluates both the inference and generative process of ActVAE and GenerativeRNN, but does not simulate the models in application, when new schedules are generated based on random samples from the latent prior. The following evaluations simulate models in application by generating synthetic samples *after* training. For the synthetic samples, schedules are generated by each model using the real sample of labels $\mathcal{S}_{\text{eval}}$ as per 5.6.

The distribution of ActVAE *synthetic schedules* can be considered as comprised of both *conditioned variation*, from the distribution of $\mathcal{S}_{\text{eval}}$ labels, and *random variation*, from the distribution of the randomly sampled latent prior. To isolate the conditional variation of synthetic schedules, i.e. ignoring random variation, we consider *expected* values from conditioned schedules. For example, we consider the expected duration of work activities in schedules belonging to employed persons versus students. Expecting, for example, that employed people will have longer work activities on average. Note that evaluation of the *distributions* of generated schedules is considered later in Section 7.4.

Figure 9 shows the modelled distributions of key expected schedule features conditional on selected labels. These are compared with the real target expected values. Specifically, we show how the *expected* values of (i) trip frequency, (ii) work frequency, (iii) shop frequency, (iv) work duration, and (v) shop duration, vary with (i) work status, (ii) household income, and (iii) age group.

In most cases, ActVAE closely follows the real target expected values, including where there is subtle and complex variation, such as for shopping activity durations by age group. The GenerativeRNN model does not have conditional capability and therefore always generates expected values close to the overall (unconditioned) expected values. The ConditionalRNN model inconsistently approximates some conditionality, but in all cases, worse than ActVAE.

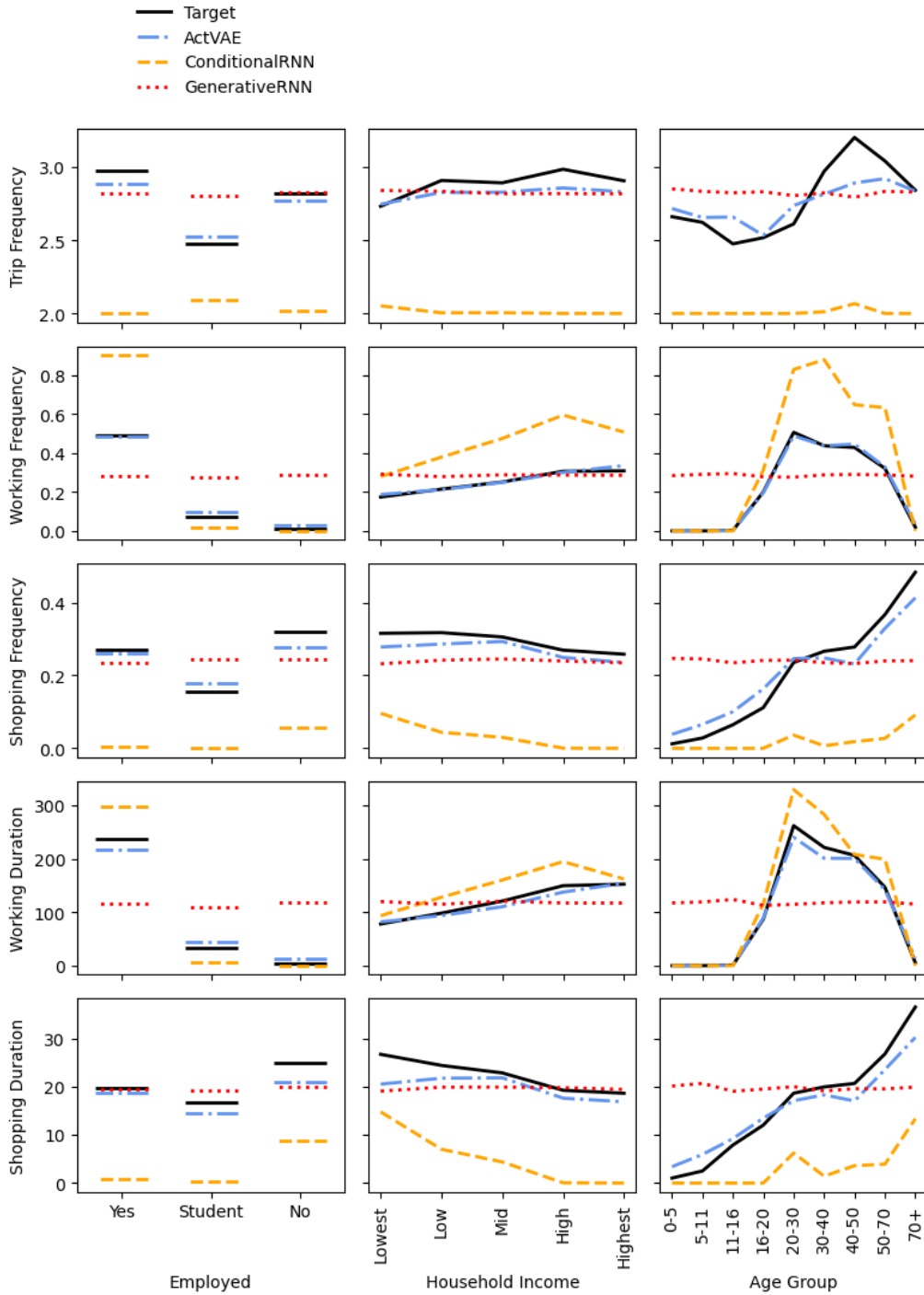


Figure 9: Expected schedule feature values by labels

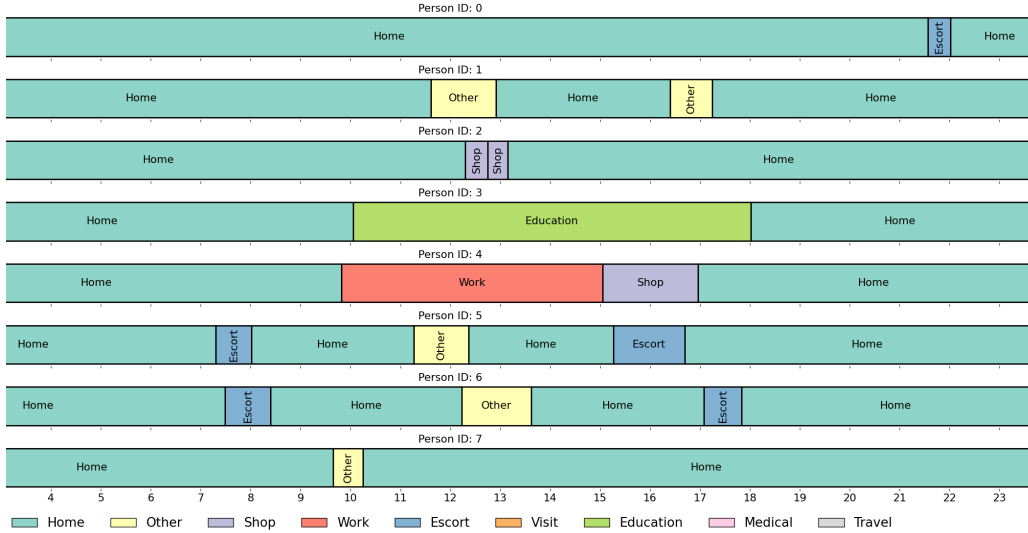


Figure 10: Example ActVAE synthetic schedules

7.3. Feasibility and creativity

Figure 10 shows a sample of synthetic schedules from ActVAE. Note that schedules are both plausible and have comparable variation to real NTS schedules (Figure 3). Table 14 presents summary evaluation metrics for feasibility and creativity. Feasibility considers the individual sample quality of output schedules. Creativity measures the ability of the model to generate diverse and novel schedules. Feasibility is reported as infeasibility and creativity as both homogeneity and conservatism, such that lower is better. Please refer to Shone and Hillel (2025) for a detailed description.

ConditionalRNN generates no infeasible schedules; however, this is at the cost of poor creativity, specifically homogeneity or lack of diversity, and, as per later sections, poor density estimation. The GenerativeRNN and ActVAE models generate infeasible schedules 2% and 3% of the time. As per Table 15, this infeasibility is due to the generation of consecutive (home, work or education) activities rather than non-home-based schedules, for which all models learn to generate exclusively home-based schedules. Note that, due to the random latent sampling process, this evaluation cannot guarantee the generative capable models will never generate non-home-based schedules, but suggests that they are extremely unlikely or infrequent.

Both the GenerativeRNN and ActVAE models are highly creative, generating very few non-unique (low homogeneity) or previously observed schedules (low conservatism). The ConditionalRNN model creates highly homogenous samples of schedules due to a lack of generative capability.

7.4. Domain-level density estimation

Table 14 presents summary evaluation metrics for joint density estimation. Lower distances are better. ActVAE is shown to have better joint density estimation than both

Table 14: Generative evaluations summary

	ConditionalRNN		GenerativeRNN		ActVAE		Unit
	dist*	var.	dist*	var.	dist*	var.	
Joint density estimation							
Participations	0.395	0.000	0.102	0.001	0.072	0.000	rate EMD
Transitions	0.023	0.000	0.009	0.000	0.005	0.000	rate EMD
Timing	0.178	0.000	0.041	0.000	0.029	0.000	days EMD
Feasibility							
Invalid	0.000	0.000	0.018	0.000	0.030	0.000	prob.
Creativity							
Homogeneity	0.994	0.000	0.037	0.000	0.024	0.000	prob.
Conservatism	0.009	0.000	0.009	0.000	0.013	0.000	prob.

* mean distances from 5 model runs

Table 15: Sample Quality Evaluations

	ConditionalRNN		GenerativeRNN		ActVAE	
	prob.*	var.	prob.*	var.	prob.*	var.
Not Home-based	0.000	0.000	0.000	0.000	0.000	0.000
Consecutive	0.000	0.000	0.018	0.000	0.030	0.000
Invalid (Combined)	0.000	0.000	0.018	0.000	0.030	0.000

* mean probability from 5 model runs

the baseline ConditionalRNN and GenerativeRNN models.

The ConditionalRNN, which approximates the most likely schedule for input labels, significantly underperforms the GenerativeRNN and ActVAE models across all the domain-level density estimations of schedule participations, transitions and timing. This suggests some combination of; (i) the model is unsuited to learning conditionality, or (ii) that conditionality alone is insufficient to explain the distribution of schedules. Based on the good conditional performance of ActVAE, which uses the same conditional architecture, and more generally, the observation of the real diversity of schedules, we propose that (ii) is primarily responsible. Or more simply, that schedules are very varied, and that explaining a lot of this variance with labels alone is hard.

We could reasonably suppose that there is a lot more conditional information available from other possible labels that we have not included, such as day of the week or weather conditions. However, our experiments in [Appendix F.3](#) suggest this is not likely to be a significant improvement. Additionally, we note that access to such descriptive features, such as weather conditions, will often be infeasible or impractical.

7.5. Label-level joint density estimation

Table 16 shows label-level joint density evaluations. Lower distances are better. Consideration of density estimation at label-level allows consideration of the quality of joint density estimation for the individual labels (age, car access, gender, income and work status).

The ConditionalRNN model performs poorly across all labels. The GenerativeRNN model, with no conditional capability, can be considered a baseline prediction, as it only uses information about the overall distribution of schedules without information about

Table 16: Label-level joint density estimation evaluations

Domain	Label	ConditionalRNN		GenerativeRNN		ActVAE	
		EMD*	var.	EMD*	var.	EMD*	var.
participations	age group	0.116	0.002	0.061	0.005	0.050	0.006
	car access	0.101	0.003	0.052	0.006	0.047	0.006
	gender	0.101	0.003	0.050	0.006	0.046	0.006
	income	0.102	0.003	0.050	0.006	0.046	0.006
	work status	0.109	0.002	0.056	0.005	0.046	0.006
transitions	age group	0.014	0.000	0.009	0.000	0.006	0.000
	car access	0.008	0.000	0.004	0.000	0.003	0.000
	gender	0.008	0.000	0.004	0.000	0.003	0.000
	income	0.011	0.000	0.005	0.000	0.004	0.000
	work status	0.011	0.000	0.006	0.000	0.004	0.000
timing	age group	0.227	0.012	0.117	0.027	0.101	0.030
	car access	0.216	0.013	0.104	0.029	0.098	0.030
	gender	0.213	0.014	0.103	0.029	0.097	0.030
	income	0.217	0.013	0.105	0.029	0.098	0.030
	work status	0.220	0.013	0.111	0.028	0.098	0.030

*EMD averaged from 5 model runs

labels. The performance of ActVAE is consistently marginally better than the generative baseline and significantly better than the conditional baseline.

Age and work status labels show the most notable improvements from the baseline generative GenerativeRNN to conditional capable ActVAE, suggesting that these labels have a *relatively strong* impact on schedules. This is sensible given, for example, that the *work status* label, particularly the *education* category, is expected to be strongly correlated with the occurrence of work and or education activities within schedules.

7.6. Category-level joint density estimation

We evaluate selected joint density estimations by selected label categories as follows: (i) Sequence lengths by employment status in [Appendix E.1](#), (ii) Activity participations by employment status in [Appendix E.2](#), (iii) Schedule transitions by gender in [Appendix E.3](#), and (iv) Activity start times and durations by car ownership in [Appendix E.4](#). Key extracts from these appendices are shown in [Table 17](#). We include both evaluation distances (EMD) and expected values for comprehensive comparison.

We show that the real or targeted impact of labels on different schedule distributions varies for different labels. For example, the real expected participation rate of *work* varies from 0.011 for unemployed persons to 0.492 for employed persons, a difference of 0.481, approximately half an additional *work* activity per day. In contrast, the expected participation rate of *escort* varies from 0.246 for unemployed persons to 0.272 for employed persons, a difference of only 0.026.

We find that ActVAE mostly outperforms the other models, especially where the importance of labels is stronger, such as for work participations by work status. Where there is more parity across categories, such as for escort participations by work status, the GenerativeRNN model will sometimes perform best simply by making a better estimation of the combined or unconditioned distribution. This is particularly notable for transitions and timings, which are relatively similar for different label categories. Whereas the

Table 17: Highlights of distribution-level joint density estimations from [Appendix E](#)

Feature	Label	Category	Real mean	ConditionalRNN mean*	ConditionalRNN EMD*	GenerativeRNN mean*	GenerativeRNN EMD*	ActVAE mean*	ActVAE EMD*	Unit
Participations										
work	work status	unemployed	0.011	0.001	0.011	0.258	0.247	0.035	0.025	rate
		student	0.073	0.006	0.067	0.251	0.178	0.064	0.013	rate
		employed	0.492	0.931	0.484	0.256	0.236	0.477	0.031	rate
		combined	0.256	0.542	0.298	0.257	0.240	0.263	0.027	rate
escort	work status	unemployed	0.246	0.008	0.238	0.260	0.063	0.233	0.036	rate
		student	0.113	0.013	0.104	0.254	0.148	0.102	0.037	rate
		employed	0.272	0.000	0.272	0.260	0.073	0.209	0.063	rate
		combined	0.256	0.006	0.248	0.259	0.070	0.218	0.050	rate
Transitions										
home-work	gender	M	0.263	0.493	0.243	0.220	0.043	0.253	0.019	rate
		F	0.216	0.454	0.251	0.220	0.025	0.226	0.014	rate
		combined	0.243	0.542	0.247	0.220	0.034	0.241	0.016	rate
home-escort	gender	M	0.180	0.000	0.180	0.216	0.056	0.169	0.024	rate
		F	0.215	0.008	0.207	0.216	0.056	0.185	0.039	rate
		combined	0.198	0.006	0.196	0.216	0.056	0.177	0.032	rate
Start times										
visit0	car access	car=yes	0.562	-	-	0.570	0.019	0.565	0.020	days
		car=no	0.553	-	-	0.570	0.024	0.565	0.018	days
		combined	0.562	-	-	0.570	0.020	0.565	0.020	days
Duration										
work0	car access	car=yes	0.339	0.220	0.137	0.304	0.040	0.314	0.031	days
		car=no	0.362	0.271	0.109	0.305	0.058	0.306	0.060	days
		combined	0.342	0.225	0.134	0.304	0.042	0.313	0.034	days

* mean density and EMD averaged from 5 model runs
- conditional model fails to generate any visit activities

generative models often perform similarly, particularly where conditionality is weak, the ConditionalRNN performs worse, often substantially.

We find that ActVAE generally slightly underestimates the magnitude of conditionality, for example, generating more, but not enough work activities for employed persons, or fewer, but still too many work activities for unemployed persons. This reflects a general bias towards the mean or unconditioned case. This is likely a result of label information leaking into generation via the latent layer, i.e. incomplete *disentanglement* as described in detail in Section 4.3. A practical implication of this is that when used for modelling new scenarios, ActVAE will be biased towards the mean, potentially underestimating the magnitude of change expected. Generally, we find this under-estimation of magnitude to be around 10%. For example, the real expected change of work participation if a person moves from unemployed to employed is 0.481, but for ActVAE only 0.442, an 8% under-estimate.

7.7. Latent-label mutual information evaluation

We use MINE by [Belghazi et al. \(2018\)](#), detailed in [Appendix D](#), for the estimation of mutual information (MI) between the real sample of schedules, real sample labels, and their learnt latent representations as per [Figure 11](#). We use these estimations to consider both (i) the performance of the GenerativeRNN and ActVAE models, and more

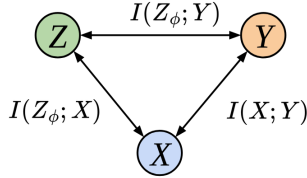


Figure 11: Summary of mutual information estimation, note that X and Y denote real samples of schedule and labels respectively, Z_ϕ denotes samples from a latent representation modelled by ϕ .

fundamentally (ii) to quantify the importance of conditional information versus random variation in modelling activity schedules.

We consider five models for latent representations; (i) Random, (ii) ActVAE, (iii) GenerativeRNN, (iv) ActVAE label encoder, and (v) ActVAE schedule encoder. The baseline *Random* embedding model verifies the MI approach, as we expect randomly generated latents to contain zero or nearly zero MI with labels or schedules. Conversely, the baseline *ActVAE label encoder* and *ActVAE schedule encoder* approximate upper bounds of the amount of MI that can be encoded, of labels and schedules, respectively. These upper bounds are achieved with random initialisations of the respective label and schedule encoder architectures, which are otherwise as described in Section 6.3.

MI results are shown in Table 18. $I(x; y)$ is an estimate of the actual MI between schedules and labels in the observed data. We can treat $I(x; y)$ as an upper bound of the amount of *useful* label information that can be embedded in latent vectors.

By comparing the estimates of embedded label information $I(z_\phi; y)$ for ActVAE and GenerativeRNN to this upper bound, we can see that ActVAE embeds approximately 37% and GenerativeRNN 75% of this upper bound into their respective latent representations. For GenerativeRNN, a purely generative VAE, higher MI is desirable, as the model has no other access to label information other than via input schedules, so it should maximise it. Conversely, for ActVAE, lower MI is desirable, as we wish to disentangle label information from the latent vectors to allow controllable generation (as per Section 4.3). We therefore show that ActVAE approximately halves the amount of label information in the latent vectors compared to the GenerativeRNN model. This likely reflects a reasonable but not complete level of disentanglement of labels from the latent vectors by ActVAE, allowing for good, but not perfect, controllable conditional generation of activity schedules.

The GenerativeRNN maximises schedule information in its latent embeddings to better reconstruct schedules. As such, we see $I(z_\phi; x)$ to be comparable to the estimated upper bound of the baseline ActVAE schedule encoder. ActVAE is similarly maximising $I(z_\phi; x)$ but independent of the label information. Consequently, the gap between $I(z_\phi; x)$ for the ActVAE and GenerativeRNN models is approximately 0.38, comparable to the amount of useful label information $I(x; y)$ (0.46), supporting the above finding of good but not complete disentanglement of label information by ActVAE.

The latent embeddings of both ActVAE and GenerativeRNN have significantly less label information $I(z_\phi; y)$ than the estimated upper bound from the ActVAE label encoder. This difference suggests that both generative latent-based models learn to ignore the majority of input label information, because it is not useful for regenerating schedules.

Table 18: Mutual information estimates; latent-labels $I(z; y)$, latent-schedules $I(z; x)$, and schedules-labels $I(x; y)$

Embedding model	$I(x; y)$ estimate		$I(z_\phi; y)$ estimate		$I(z_\phi; x)$ estimate	
	mean*	var.	mean*	var.	mean*	var.
-	0.4582	0.0006	-	-	-	-
<i>Random</i>	-	-	0.0001	0.0000	0.0082	0.0000
ActVAE	-	-	0.1702	0.0089	1.9897	0.0408
GenerativeRNN	-	-	0.3407	0.0016	2.3705	0.0316
<i>ActVAE label encoder</i>	-	-	3.9802	0.8029	-	-
<i>ActVAE schedule encoder</i>	-	-	-	-	2.2905	0.0696

* mean estimate from 5 model runs

Table 19: Average model train and generation times from 5 model runs

Model	Training*	Generation**
	Time (min)	Time (sec)
ConditionalRNN	2.60	3.32
GenerativeRNN	5.17	2.16
ActVAE	7.92	1.59

* trained until validation loss stabilises, approx. 100 epochs.

** Generation is for approx. 60,000 schedules.

This further reinforces the general finding that the usefulness of labels for explaining or modelling schedules is relatively limited compared to unexplained or random variation.

If we consider the GenerativeRNN latent as maximising both random and label information for the reconstruction of schedules, and ActVAE latent as maximising only random information, both measured using $I(z_\phi; x)$, then we can suggest that label variation is responsible for only 16% of schedule variation in MI terms $((2.3705 - 1.9897)/2.3705)$. This value is only approximate because neither model is *perfectly* maximising either random or label information in their latent embeddings.

7.8. Model run times

Table 19 shows model sizes and expected run times using an NVIDIA RTX A5000 GPU. ActVAE is trained in 8 minutes and generates approximately 60,000 schedules in 1.6 seconds. A full synthetic sample for the UK (68.3 million persons) could therefore be generated in around 30 minutes. Scaling can be trivially achieved with more and/or larger GPUs. This speed makes model and hyperparameter search cheap, moving the bottleneck in model development to the user and the evaluation tools. We provide Caveat³ to allow reproduction of results and enable extensive model and hyperparameter exploration.

7.9. Results Summary

Our conditional-generative model, ActVAE, significantly outperforms the baseline conditional model, ConditionalRNN, and to a lesser extent the baseline generative model, GenerativeRNN. We consider performances using extensive density estimation evaluation as well as supplementary metrics such as losses and mutual information. We show that the

³<https://github.com/big-ucl/caveat>

ActVAE can model conditionality, including subtle dependencies on complex inputs, such as durations of specific activities based on age, that have not been achieved by existing compositional approaches. Additionally, ActVAE learns these patterns without requiring careful model specification or feature engineering, making the model development process rapid compared to other approaches. However, we also find that ActVAE tends to underestimate the expected effect of labels by around 10% (see example in Section 7.6), most likely due to some remaining entanglement of labels and latent embedding (discussed in Section 7.7).

More broadly, we find that the variation in schedules due to labels is relatively minor compared to other unexplained or random variations. As such, the purely generative model, without access to label information, often performs similarly to the conditional capable ActVAE, and significantly better than the conditional only ConditionalRNN model at density estimation. This finding is quantified using estimations of mutual information in Section 7.7.

We additionally supplement our evaluation of ActVAE with various case studies detailed in Appendix F. In Appendix F.1 we demonstrate ActVAE on a forecasting task. Using real UK age forecasts, we show that ActVAE can be used to predict sensible changes in activity scheduling. In Appendix F.2, we explore the sensitivity of ActVAE to data availability. We show that it is likely viable with as few as 25,000 training samples, but that performance improves with more data. In Appendix F.3 we consider the sensitivity of ActVAE to the availability of input labels. We demonstrate that the approach can be simply extended for different combinations and quantities of input information. Finally, in Appendix F.4 we show that ActVAE can be trained on multiple years of data, benefiting from more data, but can then be conditioned on specific years to improve performance.

8. Conclusions and further work

We demonstrate ActVAE, an explicit generative model with both conditional and generative capability to model schedules. ActVAE combines (i) an efficient, structured latent generative approach to explicitly model random schedule variance, with (ii) conditionality, so that responses to changes in inputs can be modelled, such as rescheduling due to ageing. Through comprehensive density estimation evaluation, we show ActVAE can generate realistic schedules and realistic distributions of schedules and labels. ActVAE can be rapidly trained and can generate millions of schedules in seconds. Additionally, the model development process does not require model specifications or feature engineering and appears viable with only 25,000 schedule samples.

More generally, by comparison to a purely explicit generative and a purely conditional model that generates the most likely schedule given the input labels, we demonstrate the importance of explicitly modelling random variation in activity schedules. This is not surprising, given the huge diversity of observed activity schedules compared to available conditional information, such as socio-demographic data. We make these comparisons using both (i) density estimation for human-interpretable comparisons, such as changes in activity participations and timing, and (ii) mutual information estimation for a more formal comparison. We suggest that the *usefulness* of explicit generative processes for modelling complex human behaviours is relevant beyond activity scheduling and transport modelling.

The drawback of our deep learning approach is that ActVAE cannot be reasonably inspected to understand why it makes correct or incorrect predictions. Similarly, it cannot be trivially *tweaked* to modify specific outputs. This moves the focus of the modelling process away from theory-driven design and specification to comprehensive assurance through rapid model development and evaluation. Such rapid model development has the potential to make existing applications cheaper or allow for the consideration of more scenarios for the same cost. We hope that such *deep generative* approaches as ActVAE will facilitate modelling (i) scenarios where diversity of representation is important, (ii) increasingly large or complex scenarios that are not feasible with existing approaches, and (iii) cheaper and faster model development. We share the developed models and provide a framework for extensive model and hyperparameter exploration using Caveat⁴.

8.1. Further Work

Deep generative modelling is an enormous domain, and approaches to human activity schedule generation have only begun to be explored. We share some experiments to support the design of ActVAE, but anticipate that other approaches and architectures may be found that perform better, particularly in scenarios with much higher data availability.

We find the quantitative evaluation of the *conditional* capability of models challenging. Our core quantitative approaches; (i) measuring joint density estimation, and (ii) measuring latent disentanglement with mutual information estimation, are both influenced by the generative capability of models. Separating the conditional capability, given the relative dominance of random variation, is therefore tricky. This is a significant departure from existing approaches, which tend to focus on a limited number of key output metrics, such as trip rates by income, but generally disregard distributional effects. In some cases, this new focus towards distribution should be welcome, for example, for the more realistic representation of the real diversity of behaviour. Where key output metrics are required for evaluation, we show that these can still be extracted as expectations. However, a more general quantitative conditional evaluation process would still be welcome. A useful avenue of progress would be the adoption of supplementary classifier models for evaluation, for example, *does this schedule look like it belongs to an employed person?*

We do not *significantly* improve the quality of non-conditional generation compared to the baseline GenerativeRNN. In particular, we note that activity times, particularly short-duration structured activities, such as escort, which start at very consistent times of day, are still imperfect. This is discussed by [Shone and Hillel \(2025\)](#) and is still a potential avenue of progress. We anticipate that approaches that incorporate better time-of-day context or explicitly model time as a budget may improve this.

Our existing work is limited to 24-hour scheduling of individuals, i.e. of activity types and their timing for a single person and day. We anticipate that without dramatic increases in data availability, a combined deep generative model for activity modelling will be challenging. However, future work should explore the approach for jointly modelling households, longer durations and additional features such as trips, modes, distances and locations.

⁴<https://github.com/big-ucl/caveat>

Appendix A. The challenge of conditional VAE disentangling through a mutual information perspective

We can decompose the D_{KL} component of loss (Equation 6) as follows to include $I_\phi(z; x, y)$, i.e the mutual information between the latent vectors and labels and schedules, such that although minimising D_{KL} implies reducing label information in the latent layer (required for controllable generation), it also implies reducing information about schedules:

$$\begin{aligned}
 D_{\text{KL}}[q_\phi(z | x, y) \| p(z)] &= \mathbb{E}_{q_\phi(z, x, y)} \left[\log \frac{q_\phi(z | x, y)}{p(z)} \right] \\
 &= \mathbb{E}_{q_\phi(z, x, y)} \left[\log \frac{q_\phi(z | x, y) q_\phi(z)}{p(z) q_\phi(z)} \right] \\
 &= \mathbb{E}_{q_\phi(z, x, y)} \left[\log \frac{q_\phi(z | x, y) q_\phi(z)}{q_\phi(z) p(z)} \right] && \text{(A.1)} \\
 &= \mathbb{E}_{q_\phi(z, x, y)} \left[\log \frac{q_\phi(z | x, y)}{q_\phi(z)} \right] + \mathbb{E}_{q_\phi(z)} \left[\log \frac{q_\phi(z)}{p(z)} \right] \\
 &= I_\phi(z; x, y) + D_{\text{KL}}[q_\phi(z) \| p(z)]
 \end{aligned}$$

This highlights a key challenge of using VAEs for conditional generation: how to regularise the model such that label information is disentangled from the random latent representation.

Appendix B. Alternative generative model designs and evaluations

We compare a standard VAE (GenerativeRNN as described in Section 6) which uses a continuous latent with normally distributed prior distribution, to three alternative structured latent models:

- SWAE: Sliced Wasserstein Auto-Encoder by [Kolouri et al. \(2019\)](#). Another continuous normal latent model, but using a Wasserstein regularisation rather than KLD.
- CatVAE: Categorical reparametrisation with Gumbel-Softmax as per [Jang et al. \(2016\)](#). A categorical latent embedding of one-hot vectors, with a uniform prior distribution.
- VQVAE: Vector-Quantised VAE by [van den Oord et al. \(2017\)](#). A categorical latent embedding using token embeddings. This model does not impose a prior distribution as per the above models. Instead, we learn one using a simple generative recurrent neural network that learns to sample tokens from the latent embedding auto-regressively.

All models use the same encoder and decoder architectures and reconstruction loss as per GenerativeRNN. Latent hyperparameters are optimised to minimise loss using the Tree-structured Parzen Estimator by Optuna ([Akiba et al., 2019](#)). These hyperparameters are described at the top of Table B.20. Domain-level joint-density estimations,

Table B.20: Summary of alternative latent models

Model Description	VAE		SWAE		CatVAE		VQVAE	
Latent type	Continuous		Continuous		Categorical (one-hot)		Categorical (tokens)	
Latent prior	Normal		Normal		Uniform		Learnt	
Latent size	6		6		128x32		8x128	
Num. embeddings	-		-		32		128	
Regularisation loss	KLD		Wasserstein		Cross-entropy		Cross-entropy	
β	0.01		0.1		0.001		0.1	
Evaluations	mean*	var.	mean*	var.	mean*	var.	mean*	var.
Participations	0.102	0.001	0.140	0.000	0.429	0.000	0.286	0.017
Transitions	0.009	0.000	0.010	0.000	0.031	0.000	0.025	0.000
Timing	0.041	0.000	0.057	0.000	0.228	0.000	0.143	0.006
Feasibility	0.018	0.000	0.065	0.000	0.000	0.000	0.055	0.006
Creativity	0.015	0.000	0.013	0.000	0.500	0.000	0.392	0.018

* mean evaluations from 5 model runs

feasibility and creativity evaluations are shown at the bottom of Table B.20. We find the standard VAE to perform best at density estimation, closely followed by SWAE. Both CatVAE and VQVAE perform badly at density estimation, closely linked to their poor creativity, likely due to the unsuitability of the categorical latent prior for embedding continuous temporal information.

Appendix C. ActVAE architecture ablation study

Table C.21 summarises domain-level joint density estimation, feasibility and creativity evaluations with various ActVAE architectural ablations or changes. Key ablations include (i) loss weighting, (ii) if and where label embeddings are passed into the encoder and decoder blocks, and (iii) how, i.e. via addition versus concatenation. The baseline ActVAE architecture is primarily selected based on better joint density estimation performance (participations, transitions, and timing). However, in many cases, there is parity based on our high-level evaluations, and so a more detailed, often qualitative, review of outputs is necessary to differentiate alternative architectures. This measurement problem is discussed in Section 8.1.

Appendix D. Mutual information estimation methodology

We use MINE by Belghazi et al. (2018) for the estimation of mutual information (MI) between the real sample of schedules, labels, and inferred or learnt samples of latent representations as per Figure 11. MINE estimates MI between two random variables using the Donsker–Varadhan representation of the Kullback–Leibler divergence:

$$I(A; B) = \sup_{T \in \mathcal{T}} \mathbb{E}_{p(a,b)}[T] - \log(\mathbb{E}_{p(a)p(b)}[e^T]) \quad (\text{D.1})$$

Where T is an *optimal critic* able to distinguish between dependent and independent pairs, sometimes called the *statistics* network or model. T is approximated using a neural network trained to assign high scores to samples drawn from the joint distribution $p(a, b)$, and low scores to samples from the product of marginals $p(a)p(b)$, which represent

Table C.21: ActVAE ablations based on 5 model runs, negative evaluation change shows worse performance

	ActVAE	Ablations				
		a1	a2	a3	a4	a5
ILLW	yes	no	yes	yes	yes	yes
EHC	add	add	concat	none	none	add
EUC	none	none	none	add	none	add
DHC	add	add	concat	none	add	add
DUC	none	none	none	add	none	add
	Evaluation	Evaluation change				
Participations	0.072	-0.005	-0.003	-0.019	-0.034	-0.027
Transitions	0.005	0.000	0.000	-0.001	-0.003	-0.002
Timing	0.029	0.002	0.000	-0.013	-0.013	-0.021
Feasibility	0.030	0.012	-0.011	0.010	0.005	0.008
Creativity	0.012	-0.000	0.000	-0.001	0.000	-0.014

ILLW: Inverse label loss weight (yes/no)

EHC: Encoder hidden layer label conditionality (add/concat/none)

EUC: Encoder un-embedding layer label conditionality (add/concat/none)

DHC: Decoder hidden layer label conditionality (add/concat/none)

DUC: Decoder un-embedding layer label conditionality (add/concat/none)

independent pairs. We estimate marginals throughout by simply shuffling inputs for each batch.

We employ statistics models as per Figure D.12. All models are based on components used for the ActVAE model, detailed in Section 6.3. We use a hidden size of 256 and depth of 2 throughout for all LSTM blocks and feed-forward blocks. Feed forwards blocks are composed of two linear layers with ReLU activations. All models are trained using pairs of samples from their respective distributions. Modelled latents and their partners are inferred from a test set of schedules and labels. All models are trained on 80% of their respective samples, with 10% withheld for validation and early stopping. We report all estimates of MI in our results (Section 7.7) using a withheld 10% test set.

Appendix E. Detailed joint density estimation studies

Appendix E.1. Sequence lengths by employment status

Sequence lengths represent the number of activities, and therefore trips, in each schedule. Table E.22 shows the expected number of activities for the real and generated samples, split by employment status and combined using a weighted average. Earth Mover Distance (EMD) is also presented for each model, for a more comprehensive evaluation of quality. The expected number of activities from the real sample is approximately 3.9. This varies from the lowest, 3.475 for students, to 3.823 for unemployed people, and the highest, 3.979 for employed people. This difference shows that, in the real population, employed people are expected to participate in an additional half of an activity per day, compared to students.

The ConditionalRNN model fairly consistently generates schedules of length three, which under-represents the number of activities and trips significantly. The GenerativeRNN model more closely models sequence lengths, but without conditional capability, generates the same expected schedule lengths across the employment status groups (with

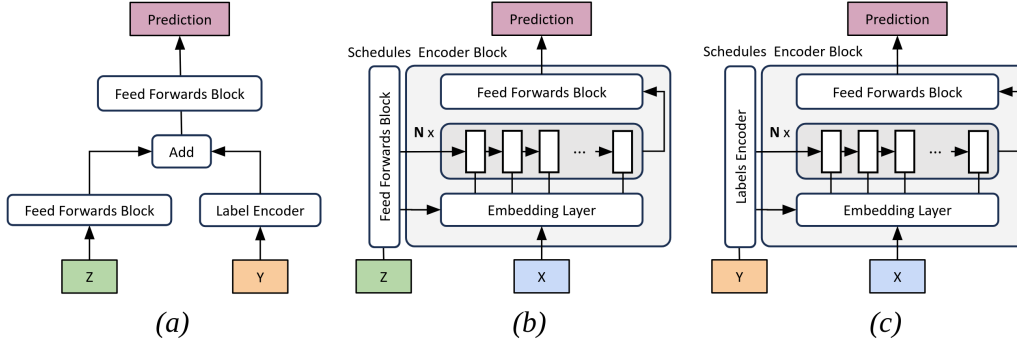


Figure D.12: Mutual information estimation (statistics) models: (a) latent-labels $I(z; y)$, (b) latent-schedules $I(z; x)$, and (c) schedules-labels $I(x; y)$

some minor random variation). Based on EMD, ActVAE captures the real distribution best, both for each employment status and on average. Note that the EMD can be lower even though the mean or expected value is closer to the real, because expected values do not consider the broader distribution. The ActVAE combined expectation of 3.813 activities is only a 3% underestimate of the number of expected activities.

Appendix E.2. Activity participations by employment status

Table E.22 also shows expected activity participations by employment status. By considering participation rates in the real sample, we can get an idea of how employment status labels impact activity participations. For example, *education* participation varies a lot (from 0.011 for employed persons to 0.511 for students, a range of 0.50) relative to *visit* participation (from 0.098 for students to 0.149 for unemployed persons, a range of only 0.05). ActVAE captures these patterns well, in most cases having the lowest distance for each participation type and employment status category.

The ConditionalRNN model sometimes captures rough patterns of activity participation based on work status, such as for education, but in most cases fails to model sensible overall rates and therefore has significantly worse distances in most cases. The GenerativeRNN model, without conditional capability, generates the same expected participations across the employment status groups (with some minor random variation). In some cases, this results in better estimation, particularly where there is little variation in the real sample, such as for visit participations.

Appendix E.3. Schedule transitions by gender

Table E.23 shows home-based activity transitions by gender. As before, the ConditionalRNN model performance is poor, and the GenerativeRNN and ActVAE models are relatively comparable. ActVAE performs best, particularly when there is more significant variation in the real sample. The greatest real differences in expected transition rates across gender are for *home-work*, which is more common for males (0.263) than for females (0.216), and *home-escort*, which is more common for females (0.215) than for males (0.180). In all cases, the ActVAE approximately models the expected relative differences between males and females, but slightly underestimates them in magnitude.

Table E.22: Distribution-level joint density estimation of sequence lengths and participations by work status, expected values and EMD from real

	Employment Status	Real expected	ConditionalRNN		GenerativeRNN		ActVAE		Unit
			expected*	EMD*	expected*	EMD*	expected*	EMD*	
Sequence Length									
	unemployed	3.823	3.003	0.880	3.781	0.168	3.762	0.138	length
	student	3.475	3.018	0.545	3.781	0.338	3.615	0.191	length
	employed	3.979	3.000	1.042	3.776	0.244	3.869	0.163	length
	combined	3.894	3.002	0.954	3.778	0.211	3.813	0.152	length
Participation									
home	unemployed	2.278	2.002	0.307	2.254	0.048	2.259	0.048	rate
	student	2.156	2.012	0.197	2.249	0.098	2.197	0.050	rate
	employed	2.339	2.000	0.371	2.253	0.092	2.328	0.055	rate
	combined	2.306	2.001	0.337	2.253	0.072	2.292	0.052	rate
other	unemployed	0.605	0.700	0.330	0.507	0.149	0.641	0.070	rate
	student	0.356	0.221	0.143	0.516	0.161	0.534	0.179	rate
	employed	0.456	0.063	0.393	0.506	0.099	0.507	0.066	rate
	combined	0.524	0.373	0.357	0.507	0.123	0.571	0.070	rate
education	unemployed	0.153	0.248	0.099	0.091	0.063	0.121	0.036	rate
	student	0.511	0.765	0.282	0.090	0.421	0.350	0.176	rate
	employed	0.011	0.002	0.009	0.092	0.081	0.009	0.003	rate
	combined	0.090	0.159	0.061	0.092	0.081	0.070	0.023	rate
work	unemployed	0.011	0.001	0.011	0.258	0.247	0.035	0.025	rate
	student	0.073	0.006	0.067	0.251	0.178	0.064	0.013	rate
	employed	0.492	0.931	0.484	0.256	0.236	0.477	0.031	rate
	combined	0.256	0.542	0.298	0.257	0.240	0.263	0.027	rate
shop	unemployed	0.320	0.045	0.275	0.229	0.091	0.284	0.046	rate
	student	0.155	0.000	0.154	0.233	0.080	0.210	0.058	rate
	employed	0.271	0.003	0.268	0.227	0.044	0.242	0.040	rate
	combined	0.291	0.030	0.269	0.228	0.067	0.261	0.043	rate
escort	unemployed	0.246	0.008	0.238	0.260	0.063	0.233	0.036	rate
	student	0.113	0.013	0.104	0.254	0.148	0.102	0.037	rate
	employed	0.272	0.000	0.272	0.260	0.073	0.209	0.063	rate
	combined	0.256	0.006	0.248	0.259	0.070	0.218	0.050	rate
visit	unemployed	0.149	0.000	0.149	0.128	0.025	0.138	0.039	rate
	student	0.098	0.000	0.098	0.128	0.044	0.134	0.057	rate
	employed	0.110	0.000	0.110	0.128	0.036	0.082	0.030	rate
	combined	0.128	0.000	0.128	0.128	0.031	0.110	0.035	rate
medical	unemployed	0.061	0.000	0.061	0.054	0.019	0.050	0.016	rate
	student	0.012	0.000	0.012**	0.060	0.048	0.025	0.014	rate
	employed	0.028	0.000	0.028	0.055	0.028	0.014	0.013	rate
	combined	0.043	0.000	0.043	0.054	0.025	0.031	0.014	rate

* mean expected values and EMD averaged from 5 model runs

** note that the ConditionalRNN model generates zero participation in visit and medical

Table E.23: Distribution-level joint density estimation of home-based transitions (2-grams) by gender, expected values and EMD to real

	Gender	Real expected	ConditionalRNN		GenerativeRNN		ActVAE		Unit
			expected*	EMD*	expected*	EMD*	expected*	EMD*	
home-work	M	0.263	0.493	0.243	0.220	0.043	0.253	0.019	rate
	F	0.216	0.454	0.251	0.220	0.025	0.226	0.014	rate
	combined	0.243	0.542	0.247	0.220	0.034	0.241	0.016	rate
home-visit	M	0.086	0.000	0.086	0.099	0.021	0.082	0.020	rate
	F	0.103	0.000	0.103	0.097	0.021	0.093	0.016	rate
	combined	0.095	0.000	0.095	0.098	0.021	0.087	0.018	rate
home-shop	M	0.213	0.013	0.200	0.166	0.047	0.179	0.039	rate
	F	0.228	0.032	0.196	0.167	0.062	0.194	0.040	rate
	combined	0.221	0.030	0.198	0.167	0.054	0.187	0.039	rate
home-other	M	0.460	0.360	0.099	0.414	0.106	0.498	0.048	rate
	F	0.442	0.370	0.090	0.417	0.099	0.475	0.044	rate
	combined	0.450	0.373	0.095	0.415	0.102	0.486	0.046	rate
home-med.	M	0.033	0.000	0.033	0.053	0.020	0.027	0.009	rate
	F	0.041	0.000	0.041	0.053	0.016	0.035	0.011	rate
	combined	0.038	0.000	0.038	0.053	0.018	0.031	0.010	rate
home-escort	M	0.180	0.000	0.180	0.216	0.056	0.169	0.024	rate
	F	0.215	0.008	0.207	0.216	0.056	0.185	0.039	rate
	combined	0.198	0.006	0.196	0.216	0.056	0.177	0.032	rate
home-edu.	M	0.086	0.134	0.049	0.085	0.017	0.066	0.021	rate
	F	0.086	0.137	0.052	0.085	0.017	0.064	0.023	rate
	combined	0.086	0.159	0.051	0.085	0.017	0.066	0.022	rate

* mean expected values and EMD averaged from 5 model runs

GenerativeRNN notably performs best at home-education transitions where there is no or very little conditionality in the real sample (both males and females have an expected rate of 0.086 in the real sample). In this case, there is no advantage to the ActVAE conditional capability, and the GenerativeRNN model simply has better aggregate density estimation.

Appendix E.4. Selected activity start times and durations by car ownership

Table E.24 evaluates selected activity start times and durations by car ownership. The *unknown* car ownership category is not shown for clarity. Activities are enumerated by their occurrence in a schedule. For example, *home0* denotes the first home activity in a schedule, and *home1*, the second. For the real sample, car ownership appears to have the most impact on the duration of *visit0* activities. Car owners have a mean *visit0* duration of 0.124 days (approximately 3 hours) and non-car owners of 0.168 (4 hours). In most other cases, the expected variation of activity start times and durations due to car ownership is under an hour. This lack of variation is likely why the GenerativeRNN and ActVAE performance is more comparable than for the above participation and transition evaluations. However, where there is more significant variation due to conditionality, such as for the duration of *visit0*, the ActVAE performs best.

The greatest evaluation distance for ActVAE is for the duration of *work0* activities without car ownership. The real and modelled expected durations of these activities are 0.362 and 0.306 days, a difference of approximately 80 minutes, showing that the ActVAE is typically underestimating *work0* durations by around 14%. The minimum (non-zero) evaluation distance for the ActVAE is for the duration of *shop0* activities with

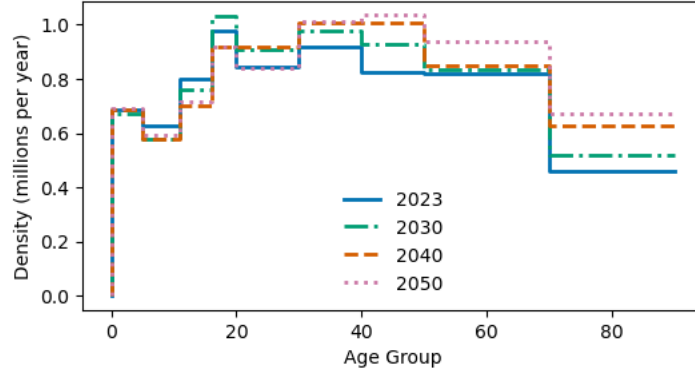


Figure F.13: Nomis age projections

car ownership. However, taking into account the shorter duration of *shop0* activities, the expected discrepancy is a 10% overestimation of duration. The size of this discrepancy is somewhat consistent across both the GenerativeRNN and ActVAE models, underestimating long activities and overestimating short activities by around 10% of real expected durations.

Appendix F. Supplementary Case Studies

We demonstrate ActVAE in several case studies, which provide additional information about expected performance when applied to other data and scenarios.

Appendix F.1. Forecasting demonstration

To illustrate the application of ActVAE, we model schedules for 2023 (baseline), 2030, 2040, and 2050 scenarios, based on projected changes to population size and age according to Nomis projections⁵, summarised in Figure F.13.

ActVAE is trained using the real (2023) NTS sample, training takes approximately 5 minutes. This model is then used to generate 1% samples, around 750,000 schedules, conditional on age group for the 2023, 2030, 2040 and 2050 scenarios. The model takes approximately 15 seconds to generate schedules.

Table F.25 presents the resulting changes to activity participations for each scenario compared to the baseline 2023 scenario. Based on expected activity sequence length, overall expected activity levels of the ageing populations are relatively stable. However, fewer young people result in a drop in education and medical activities. Conversely, the ageing population is more likely to shop, work or visit.

Appendix F.2. Data availability case study

We evaluate the performance of ActVAE in scenarios with different data availability. NTS data from 2019 to 2023 is combined and then randomly sampled to create five

⁵<https://www.nomisweb.co.uk/datasets/ppsyoa>

Table E.24: Distribution-level joint density estimation of selected activity start times and durations by car ownership, expected values and EMD to real

Car Ownership		Real expected	ConditionalRNN expected*	EMD*	GenerativeRNN expected*	EMD*	ActVAE expected*	EMD*	Unit
Start Times									
work0	car=yes	0.362	0.510	0.159	0.385	0.033	0.384	0.024	days
	car=no	0.382	0.473	0.114	0.385	0.023	0.414	0.033	days
	combined	0.365	0.506	0.155	0.385	0.031	0.387	0.025	days
visit0	car=yes	0.562	-	-	0.570	0.019	0.565	0.020	days
	car=no	0.553	-	-	0.570	0.024	0.565	0.018	days
	combined	0.562	-	-	0.570	0.020	0.565	0.020	days
shop0	car=yes	0.532	0.335	0.276	0.545	0.023	0.547	0.018	days
	car=no	0.515	0.516	0.085	0.545	0.040	0.547	0.036	days
	combined	0.530	0.519	0.239	0.545	0.025	0.546	0.020	days
home1	car=yes	0.622	0.709	0.118	0.636	0.019	0.633	0.015	days
	car=no	0.657	0.689	0.074	0.636	0.026	0.654	0.017	days
	combined	0.626	0.706	0.113	0.636	0.020	0.636	0.015	days
home0	car=yes	0.000	0.000	0.000	0.000	0.000	0.000	0.000	days
	car=no	0.000	0.000	0.000	0.000	0.000	0.000	0.000	days
	combined	0.000	0.000	0.000	0.000	0.000	0.000	0.000	days
education0	car=yes	0.359	0.481	0.125	0.386	0.038	0.379	0.022	days
	car=no	0.379	0.447	0.077	0.389	0.027	0.408	0.032	days
	combined	0.362	0.477	0.119	0.387	0.037	0.383	0.024	days
Durations									
work0	car=yes	0.339	0.220	0.137	0.304	0.040	0.314	0.031	days
	car=no	0.362	0.271	0.109	0.305	0.058	0.306	0.060	days
	combined	0.342	0.225	0.134	0.304	0.042	0.313	0.034	days
visit0	car=yes	0.124	-	-	0.137	0.023	0.160	0.037	days
	car=no	0.168	-	-	0.137	0.034	0.165	0.018	days
	combined	0.128	-	-	0.137	0.024	0.160	0.035	days
shop0	car=yes	0.052	0.068	0.064	0.069	0.022	0.057	0.011	days
	car=no	0.075	0.097	0.047	0.069	0.018	0.066	0.013	days
	combined	0.054	0.098	0.061	0.069	0.021	0.058	0.011	days
home1	car=yes	0.278	0.291	0.105	0.281	0.020	0.281	0.012	days
	car=no	0.302	0.311	0.069	0.281	0.032	0.283	0.027	days
	combined	0.281	0.293	0.101	0.281	0.021	0.281	0.014	days
home0	car=yes	0.454	0.530	0.115	0.464	0.019	0.464	0.020	days
	car=no	0.467	0.492	0.087	0.466	0.019	0.484	0.027	days
	combined	0.456	0.526	0.112	0.464	0.019	0.467	0.021	days
education0	car=yes	0.302	0.231	0.080	0.267	0.041	0.283	0.027	days
	car=no	0.288	0.248	0.061	0.268	0.028	0.264	0.030	days
	combined	0.300	0.233	0.077	0.267	0.040	0.280	0.028	days

* mean expected values and EMD averaged from 5 model runs

- ConditionalRNN fails to generate any visit activities

Table F.25: Changes, compared to 2023, of expected activity participations using Nomis age projections

		2023	Δ 2030	Δ 2040	Δ 2050
Sequence Length		3.830	+0.53%	+0.59%	+0.68%
Participation rate	home	2.257	-0.29%	-0.24%	-0.18%
	other	0.521	-1.15%	-1.13%	-1.12%
	shop	0.292	+7.16%	+8.97%	+9.83%
	work	0.264	+0.73%	+0.99%	+0.96%
	escort	0.214	+2.73%	+2.06%	+1.95%
	visit	0.177	+10.63%	+10.90%	+11.16%
	education	0.068	-15.61%	-21.80%	-23.52%
	medical	0.036	-11.59%	-10.15%	-9.48%

Table F.26: Sample Sizes Scenario Evaluation Summary

	200k	100k	50k	25k	12.5k
Joint Density Estimation					
Participations	0.084	0.080	0.089	0.151	0.197
Transitions	0.008	0.008	0.010	0.010	0.021
Timing	0.030	0.030	0.039	0.049	0.068
Feasibility	0.011	0.010	0.022	0.040	0.108
Creativity	0.008	0.005	0.002	0.002	0.002

scenarios with real samples of size 200k, 100k, 50k, 25k, and 12.5k. ActVAE is trained on these samples and then evaluated. We use labels from the 25k sample for generation, so that scenario evaluations are comparable.

Table F.26 summarises results from this experiment. We see a clear trend in worsening density estimation and sample quality as the sample size decreases. We suggest a minimum real sample size of 25,000 schedules for application in a modelling framework. Conversely, we see that larger samples result in both better density destination and feasibility.

Appendix F.3. Labels availability case study

To consider the impact of the amount of conditional information on ActVAE, specifically to see if adding more labels improves density estimation, we evaluate five scenarios with 1, 2, 4, 8 and 16 labels from the NTS individual and households tables as per Table F.27. For each scenario, ActVAE is trained using the modified real samples and then evaluated. Note that the evaluation of joint density estimation considers work status only, as this is the only label consistently available across all models.

Evaluations in Table F.28 show some evidence that scenarios with more labels perform worse at participation density estimation. Further inspection of density estimation suggests this is caused by a degradation in the performance of the generative rather than conditional process within the model. This can be mitigated, for example, by throttling the transfer of label information by reducing the label hidden latent size H . However, the impact is minimal, such that a pragmatic modeller might simply include all available labels and skip the time-consuming process of feature selection and engineering. Alternatively, a modeller may only include labels that are required as part of the broader modelling process and allow the generative model process to “fill in the gaps”.

Table F.27: Labels Scenarios

	L=1	L=2	L=4	L=8	L=16
Work Status	✓	✓	✓	✓	✓
Area	-	✓	✓	✓	✓
Age Group	-	-	✓	✓	✓
Mobility	-	-	✓	✓	✓
Income	-	-	-	✓	✓
Education	-	-	-	✓	✓
Ethnicity	-	-	-	✓	✓
Gender	-	-	-	✓	✓
Car Access	-	-	-	-	✓
License	-	-	-	-	✓
Working from Home	-	-	-	-	✓
Wheelchair User	-	-	-	-	✓
Ticket Holder	-	-	-	-	✓
Health	-	-	-	-	✓
Blue Badge Holder	-	-	-	-	✓
Household Licenses	-	-	-	-	✓

Table F.28: Conditional Labels Scenario Evaluation Summary

	L=1	L=2	L=4	L=8	l=16
Joint density estimation (joint schedules and work status only)					
Participations	0.060	0.066	0.061	0.083	0.105
Transitions	0.005	0.006	0.004	0.006	0.005
Timing	0.026	0.029	0.032	0.032	0.035
Feasibility	0.014	0.037	0.032	0.024	0.009
Creativity	0.024	0.024	0.021	0.017	0.017

Table F.29: Foundational Model Evaluation Summary

	Base	Foundational Base	Foundational
Training data	2023	2019-2023	2019-2023
Conditioned on	2023	2019-2023	2023
Joint density estimation			
Participations	0.072	0.050	0.046
Transitions	0.005	0.003	0.002
Timing	0.029	0.019	0.016
Feasibility	0.030	0.011	0.007
Creativity	0.023	0.020	0.023

Appendix F.4. Foundational model case study

Finally, we consider the ability of ActVAE to use training data from alternative contexts. Specifically, we train a *Foundational* model on NTS data from 2019 to 2023 and then condition the generation on 2023 only using a label for each year. Table F.29 compares evaluations to (i) the *Base* ActVAE model (trained on 2023 only), and (ii) a *Foundational Base* model, trained on 2019 to 2023 data but not conditioned on 2023 alone. The *Foundational* model outperforms both base models. This demonstrates that models can benefit from more data, even from different years (including Covid years in this case), and that this can be further improved through conditioning. This approach demonstrates a simple way to leverage data from other years and perhaps geographies or populations, provided consistent labels can be created.

CRedit authorship contribution statement

Fred Shone: Conceptualization, Methodology, Software, Formal analysis, Investigation, Writing – original draft, Writing – review & editing, Visualization. **Tim Hillel:** Conceptualization, Methodology, Writing - review & editing, Supervision, Funding acquisition.

Acknowledgments

This work was supported by the Engineering and Physical Sciences Research Council (EPSRC) [grant numbers EP/T517793/1 and EP/W524335/1].

References

- Akiba, T., Sano, S., Yanase, T., Ohta, T., Koyama, M., 2019. Optuna: A next-generation hyperparameter optimization framework, in: Proceedings of the 25th ACM SIGKDD International Conference on Knowledge Discovery and Data Mining.
- Apellaniz, P.A., Parras, J., Zazo, S., 2024. An improved tabular data generator with vae-gmm integration, in: 2024 32nd European Signal Processing Conference (EUSIPCO), pp. 1886–1890. doi:10.23919/EUSIPCO63174.2024.10715230.
- Badu-Marfo, G., Farooq, B., Patterson, Z., 2020. A differentially private multi-output deep generative networks approach for activity diary synthesis. [arXiv:2012.14574](https://arxiv.org/abs/2012.14574).

- Belghazi, M.I., Baratin, A., Rajeshwar, S., Ozair, S., Bengio, Y., Courville, A., Hjelm, D., 2018. Mutual information neural estimation, in: Dy, J., Krause, A. (Eds.), Proceedings of the 35th International Conference on Machine Learning, PMLR. pp. 531–540. URL: <https://proceedings.mlr.press/v80/belghazi18a.html>.
- Bond-Taylor, S., Leach, A., Long, Y., Willcocks, C.G., 2022. Deep generative modelling: A comparative review of vaes, gans, normalizing flows, energy-based and autoregressive models. *IEEE Transactions on Pattern Analysis and Machine Intelligence* 44, 7327–7347. doi:10.1109/TPAMI.2021.3116668.
- Bradley, M., Bowman, J.L., Griesenbeck, B., 2010. SACSIM: An applied activity-based model system with fine-level spatial and temporal resolution. *Journal of Choice Modelling* 3, 5–31. URL: <https://www.sciencedirect.com/science/article/pii/S1755534513700277>, doi:[https://doi.org/10.1016/S1755-5345\(13\)70027-7](https://doi.org/10.1016/S1755-5345(13)70027-7).
- Brown, T., Mann, B., Ryder, N., Subbiah, M., Kaplan, J.D., Dhariwal, P., Neelakantan, A., Shyam, P., Sastry, G., Askell, A., Agarwal, S., Herbert-Voss, A., Krueger, G., Henighan, T., Child, R., Ramesh, A., Ziegler, D., Wu, J., Winter, C., Hesse, C., Chen, M., Sigler, E., Litwin, M., Gray, S., Chess, B., Clark, J., Berner, C., McCandlish, S., Radford, A., Sutskever, I., Amodei, D., 2020. Language models are few-shot learners, in: Larochelle, H., Ranzato, M., Hadsell, R., Balcan, M., Lin, H. (Eds.), *Advances in Neural Information Processing Systems*, Curran Associates, Inc. pp. 1877–1901. URL: https://proceedings.neurips.cc/paper_files/paper/2020/file/1457c0d6bfc4967418bfb8ac142f64a-Paper.pdf.
- Burgess, C.P., Higgins, I., Pal, A., Matthey, L., Watters, N., Desjardins, G., Lerchner, A., 2018. Understanding disentangling in β -VAE. [arXiv:1804.03599](https://arxiv.org/abs/1804.03599).
- Chen, X., Duan, Y., Houthoofd, R., Schulman, J., Sutskever, I., Abbeel, P., 2016. Infogan: Interpretable representation learning by information maximizing generative adversarial nets, in: Lee, D., Sugiyama, M., Luxburg, U., Guyon, I., Garnett, R. (Eds.), *Advances in Neural Information Processing Systems*, Curran Associates, Inc. URL: https://proceedings.neurips.cc/paper_files/paper/2016/file/7c9d0b1f96aebd7b5eca8c3edaa19ebb-Paper.pdf.
- Deng, H., Pan, T., Diao, H., Luo, Z., Cui, Y., Lu, H., Shan, S., Qi, Y., Wang, X., 2025. Autoregressive video generation without vector quantization, in: *International Conference on Learning Representations (ICLR)*. URL: <https://openreview.net/forum?id=JE9tCwe3lp>.
- Devlin, J., Chang, M.W., Lee, K., Toutanova, K., 2018. BERT: Pre-training of deep bidirectional transformers for language understanding. *arXiv preprint arXiv:1810.04805*.
- Diamantis, D.E., Gatoula, P., Iakovidis, D.K., 2022. Endovae: Generating endoscopic images with a variational autoencoder, in: *2022 IEEE 14th Image, Video, and Multidimensional Signal Processing Workshop (IVMSP)*, pp. 1–5. doi:10.1109/IVMSP54334.2022.9816329.
- Goodfellow, I., Pouget-Abadie, J., Mirza, M., Xu, B., Warde-Farley, D., Ozair, S., Courville, A., Bengio, Y., 2014. Generative adversarial nets, in: Ghahramani, Z., Welling, M., Cortes, C., Lawrence, N., Weinberger, K. (Eds.), *Advances in Neural Information Processing Systems*, Curran Associates, Inc. URL: http://proceedings.neurips.cc/paper_files/paper/2014/file/f033ed80deb0234979a61f95710dbe25-Paper.pdf.
- Hafezi, M.H., Daisy, N.S., Millward, H., Liu, L., 2021. Ensemble learning activity scheduler for activity based travel demand models. *Transportation Research Part C: Emerging Technologies* 123, 102972. URL: <https://www.sciencedirect.com/science/article/pii/S0968090X21000097>, doi:<https://doi.org/10.1016/j.trc.2021.102972>.
- Higgins, I., Matthey, L., Pal, A., Burgess, C.P., Glorot, X., Botvinick, M.M., Mohamed, S., Lerchner, A., 2016. beta-vae: Learning basic visual concepts with a constrained variational framework, in: *International Conference on Learning Representations*. URL: <https://api.semanticscholar.org/CorpusID:46798026>.
- Ho, J., Jain, A., Abbeel, P., 2020. Denoising diffusion probabilistic models, in: Larochelle, H., Ranzato, M., Hadsell, R., Balcan, M., Lin, H. (Eds.), *Advances in Neural Information Processing Systems*, Curran Associates, Inc. pp. 6840–6851. URL: <https://proceedings.neurips.cc/paper/2020/hash/4c5bcfec8584af0d967f1ab10179ca4b-Abstract.html>.
- Hochreiter, S., Schmidhuber, J., 1997. Long Short-Term Memory. *Neural Computation* 9, 1735–1780. doi:10.1162/neco.1997.9.8.1735.
- Jang, E., Gu, S., Poole, B., 2016. Categorical reparameterization with gumbel-softmax doi:10.48550/arXiv.1611.01144.
- Kebaili, A., Lapuyade-Lahorgue, J., Vera, P., Ruan, S., 2024. Discriminative hamiltonian variational autoencoder for accurate tumor segmentation in data-scarce regimes. *Neurocomputing* 606, 128360. doi:10.1016/j.neucom.2024.128360.
- Khan, N.A., Habib, M.A., 2023. Microsimulation of activity generation, activity scheduling and shared

- travel choices within an activity-based travel demand modelling system. *Travel Behaviour and Society* 32, 100590. doi:<https://doi.org/10.1016/j.tbs.2023.100590>.
- Kim, E.J., Kim, D.K., Sohn, K., 2022. Imputing qualitative attributes for trip chains extracted from smart card data using a conditional generative adversarial network. *Transportation Research Part C: Emerging Technologies* 137, 103616. doi:[10.1016/j.trc.2022.103616](https://doi.org/10.1016/j.trc.2022.103616).
- Kingma, D.P., Rezende, D.J., Mohamed, S., Welling, M., 2014. Semi-supervised learning with deep generative models, in: Ghahramani, Z., Welling, M., Cortes, C., Lawrence, N., Weinberger, K. (Eds.), *Advances in Neural Information Processing Systems*, Curran Associates, Inc. URL: https://proceedings.neurips.cc/paper_files/paper/2014/file/6d42b1217a6996997ead5a8398c1f944-Paper.pdf.
- Kingma, D.P., Welling, M., 2013. Auto-Encoding Variational Bayes. doi:[10.48550/arXiv.1312.6114](https://doi.org/10.48550/arXiv.1312.6114), [arXiv:1312.6114](https://arxiv.org/abs/1312.6114).
- Kolouri, S., Pope, P.E., Martin, C.E., Rohde, G.K., 2019. Sliced wasserstein auto-encoders, in: *International Conference on Learning Representations*. URL: <https://openreview.net/forum?id=H1xaJn05FQ>.
- Koushik, A., Manoj, M., Nezamuddin, N., Prathosh, AP., 2023. Activity Schedule Modeling Using Machine Learning. *Transportation Research Record* 2677, 1–23. doi:[10.1177/03611981231155426](https://doi.org/10.1177/03611981231155426).
- Larsen, A.B.L., Sønderby, S.K., Larochelle, H., Winther, O., 2016. Autoencoding beyond pixels using a learned similarity metric, in: Balcan, M.F., Weinberger, K.Q. (Eds.), *Proceedings of The 33rd International Conference on Machine Learning*, PMLR, New York, New York, USA. pp. 1558–1566. URL: <https://proceedings.mlr.press/v48/larsen16.html>.
- Lee, I.G., Oh, J.Y., Yu, H.J., Kim, J.H., Eom, K.D., Jeong, J.H., 2024. Generative active learning with variational autoencoder for radiology data generation in veterinary medicine, pp. 626–631. doi:[10.1109/CAI59869.2024.00123](https://doi.org/10.1109/CAI59869.2024.00123).
- Liu, K., Jin, X., Cheng, S., Gao, S., Yin, L., Lu, F., 2024. Act2loc: a synthetic trajectory generation method by combining machine learning and mechanistic models. *International Journal of Geographical Information Science* 38, 407–431. URL: <https://doi.org/10.1080/13658816.2023.2292570>, doi:[10.1080/13658816.2023.2292570](https://doi.org/10.1080/13658816.2023.2292570).
- Lucas, T., Shmelkov, K., Alahari, K., Schmid, C., Verbeek, J., 2019. Adaptive density estimation for generative models, in: Wallach, H., Larochelle, H., Beygelzimer, A., d'Alché-Buc, F., Fox, E., Garnett, R. (Eds.), *Advances in Neural Information Processing Systems*, Curran Associates, Inc. URL: https://proceedings.neurips.cc/paper_files/paper/2019/file/959ab9a0695c467e7caf75431a872e5c-Paper.pdf.
- Manser, P., Haering, T., Hillel, T., Pougala, J., Krueger, R., Bierlaire, M., 2021. Resolving temporal scheduling conflicts in activity-based modelling. URL: <https://transp-or.epfl.ch/documents/technicalReports/ManserEtAl2021.pdf>.
- Mescheder, L., Nowozin, S., Geiger, A., 2017. Adversarial variational bayes: Unifying variational autoencoders and generative adversarial networks, in: Precup, D., Teh, Y.W. (Eds.), *Proceedings of the 34th International Conference on Machine Learning*, PMLR. pp. 2391–2400. URL: <https://proceedings.mlr.press/v70/mescheder17a.html>.
- Molnár, S., Tamas, L., 2024. Variational autoencoders for 3d data processing. *Artificial Intelligence Review* 57. doi:[10.1007/s10462-023-10687-x](https://doi.org/10.1007/s10462-023-10687-x).
- Nayak, S., Pandit, D., 2023. A joint and simultaneous prediction framework of weekday and weekend daily-activity travel pattern using conditional dependency networks. *Travel Behaviour and Society* 32, 100595. URL: <https://www.sciencedirect.com/science/article/pii/S2214367X23000467>, doi:<https://doi.org/10.1016/j.tbs.2023.100595>.
- van den Oord, A., Vinyals, O., Kavukcuoglu, k., 2017. Neural discrete representation learning, in: Guyon, I., Luxburg, U.V., Bengio, S., Wallach, H., Fergus, R., Vishwanathan, S., Garnett, R. (Eds.), *Advances in Neural Information Processing Systems*, Curran Associates, Inc. URL: https://proceedings.neurips.cc/paper_files/paper/2017/file/7a98af17e63a0ac09ce2e96d03992fbc-Paper.pdf.
- Oord, A.V.D., Kalchbrenner, N., Espeholt, L., Kavukcuoglu, K., Vinyals, O., Graves, A., 2016. Conditional image generation with pixelcnn decoders. *ArXiv abs/1606.05328*.
- Pougala, J., Hillel, T., Bierlaire, M., 2023. Oasis: Optimisation-based activity scheduling with integrated simultaneous choice dimensions. *Transportation Research Part C: Emerging Technologies* 155, 104291. doi:<https://doi.org/10.1016/j.trc.2023.104291>.
- Rezende, D., Mohamed, S., 2015. Variational inference with normalizing flows, in: Bach, F., Blei, D. (Eds.), *Proceedings of the 32nd International Conference on Machine Learning*, PMLR, Lille, France. pp. 1530–1538. URL: <https://proceedings.mlr.press/v37/rezende15.html>.
- Rezende, D.J., Mohamed, S., Wierstra, D., 2014. Stochastic backpropagation and approximate inference

- in deep generative models, in: Xing, E.P., Jebara, T. (Eds.), Proceedings of the 31st International Conference on Machine Learning, PMLR, Beijing, China. pp. 1278–1286. URL: <https://proceedings.mlr.press/v32/rezende14.html>.
- Rezvany, N., Bierlaire, M., Hillel, T., . Simulating intra-household interactions for in- and out-of-home activity scheduling 157, 104362. URL: <https://www.sciencedirect.com/science/article/pii/S0968090X23003522>, doi:10.1016/j.trc.2023.104362.
- Sajjadi, M.S.M., Bachem, O., Lucic, M., Bousquet, O., Gelly, S., 2018. Assessing generative models via precision and recall, in: Bengio, S., Wallach, H., Larochelle, H., Grauman, K., Cesa-Bianchi, N., Garnett, R. (Eds.), Advances in Neural Information Processing Systems, Curran Associates, Inc. URL: https://proceedings.neurips.cc/paper_files/paper/2018/file/f7696a9b362ac5a51c3dc8f098b73923-Paper.pdf.
- Salvadé, N., Hillel, T., 2025. RUMBoost: Gradient boosted random utility models. URL: <https://www.sciencedirect.com/science/article/pii/S0968090X24004182>, doi:<https://doi.org/10.1016/j.trc.2024.104897>.
- Sener, I.N., Bhat, C.R., Copperman, R., Srinivasan, S., Guo, J.Y., Pinjari, A., Eluru, N., 2006. Activity-based travel-demand analysis for metropolitan areas in Texas: CEMDAP models, framework, software architecture and application results. Technical Report. Midwest Regional University Transportation Center.
- Shone, F., Chatzioannou, T., Pickering, B., Kozłowska, K., Fitzmaurice, M., 2024. PAM: Population Activity Modeller. Journal of Open Source Software 9, 6097. doi:10.21105/joss.06097.
- Shone, F., Hillel, T., 2025. Synthesising activity participations and scheduling with deep generative machine learning. Transportation Research Part C: Emerging Technologies 179, 105273. URL: <https://www.sciencedirect.com/science/article/pii/S0968090X25002773>, doi:<https://doi.org/10.1016/j.trc.2025.105273>.
- Sutskever, I., Vinyals, O., Le, Q.V., 2014. Sequence to sequence learning with neural networks, in: Ghahramani, Z., Welling, M., Cortes, C., Lawrence, N., Weinberger, K. (Eds.), Advances in Neural Information Processing Systems, Curran Associates, Inc. URL: https://proceedings.neurips.cc/paper_files/paper/2014/file/5a18e133cbf9f257297f410bb7eca942-Paper.pdf.
- Tang, Z., Gu, S., Bao, J., Chen, D., Wen, F., 2022. Improved vector quantised diffusion models. ArXiv abs/2205.16007. URL: <https://api.semanticscholar.org/CorpusID:249209888>.
- Vazquez, B., Hevia, N., Perez-Gonzalez, J., Haro, P., 2025. Weighted-vae: A deep learning approach for multimodal data generation applied to experimental t. cruzi infection. PLOS ONE 20. doi:10.1371/journal.pone.0315843.
- Xu, T., Zhang, P., Huang, Q., Zhang, H., Gan, Z., Huang, X., He, X., 2018. AttnGAN: Fine-grained text to image generation with attentional generative adversarial networks, in: 2018 IEEE/CVF Conference on Computer Vision and Pattern Recognition, pp. 1316–1324. doi:10.1109/CVPR.2018.00143.